Cranial ontogenetic variation in early saurischians and the role of heterochrony in the diversification of predatory dinosaurs

Christian Foth, Brandon P Hedrick, Martin D Ezcurra

Non-avian saurischian skulls underwent at least 165 million years of evolution and shapes varied from elongated skulls, such as in the theropod *Coelophysis*, to short and box-shaped skulls, such as in the sauropod *Camarasaurus*. A number of factors have long been considered to drive skull shape, including phylogeny, dietary preferences and functional constraints. However, heterochrony is increasingly being recognized as an important factor in dinosaur evolution. In order to quantitatively analyse the impact of heterochrony on saurischian skull shape, we analysed five ontogenetic trajectories using two-dimensional geometric morphometrics in a phylogenetic framework. This allowed for the comparative investigation of main ontogenetic shape changes and the evaluation of how heterochrony affected skull shape through both ontogenetic and phylogenetic trajectories. Using principal component analyses and multivariate regressions, it was possible to quantify different ontogenetic trajectories and evaluate them for evidence of heterochronic events allowing testing of previous hypotheses on cranial heterochrony in saurischians. We found that the skull shape of the hypothetical ancestor of Saurischia likely led to basal Sauropodomorpha through paedomorphosis, and to basal Theropoda mainly through peramorphosis. Paedomorphosis then led from Orionides to Avetheropoda, indicating that the paedomorphic trend previously found in advanced coelurosaurs may extend back into the early evolution of Avetheropoda. Not only are changes in saurischian skull shape complex due to the large number of factors that affected it, but heterochrony itself is complex, with a number of possible reversals throughout non-avian saurischian evolution. In general, the sampling of complete ontogenetic trajectories including early juveniles is considerably lower than the sampling of single adult or subadult individuals, which is a major impediment to the study of heterochrony on non-avian dinosaurs. Thus, the current work represents an exploratory analysis. To better understand the cranial ontogeny and the impact of heterochrony on skull evolution in saurischians, the data set that we present here must be expanded and complemented with further sampling from future fossil discoveries, especially of juvenile individuals.

Cranial ontogenetic variation in early saurischians and the role of heterochrony in the diversification of predatory dinosaurs

Christian Foth[1,2,3], Brandon P. Hedrick[4,5], Martín D. Ezcurra[2,6,7]

[1] SNBS, Bayerische Staatssammlung für Paläontologie und Geologie, Richard Wagner-Str. 10, D-80333 München

[2] Department of Earth and Environmental Sciences, Ludwig-Maximilians-Universität, Richard-Wagner-Str. 10, D-80333 München, Germany

[3] Department of Geosciences, University of Fribourg/Freiburg, Chemin du Musée 6, 1700 Fribourg, Switzerland

[4] Department of Earth and Environmental Science, University of Pennsylvania, 251 Hayden Hall, 240 S 33rd Street, Philadelphia, PA 19104, USA

[5] Department of Biology, University of Massachusetts, 321 Morrill Science Center, 611 North Pleasant Street, Amherst, MA 01003, USA

[6] School of Geography, Earth and Environmental Sciences, University of Birmingham, Edgbaston, Birmingham B15 2TT, UK

[7] Sección Paleontología de Vertebrados, Museo Argentino de Ciencias Naturales "Bernardino Rivadavia", Buenos Aires C1405DJR, Argentina

Correspondence: Christian Foth, Department of Geosciences, University of Fribourg/Freiburg, Chemin du Musée 6, 1700 Fribourg, Switzerland

Tel.: +41 26 300 8944

e-mail: christian.foth@gmx.net

Short title: Heterochrony in early saurischian skulls

Abstract

Non-avian saurischian skulls underwent at least 165 million years of evolution and shapes varied from elongated skulls, such as in the theropod *Coelophysis*, to short and box-shaped skulls, such as in the sauropod *Camarasaurus*. A number of factors have long been considered to drive skull shape, including phylogeny, dietary preferences and functional constraints. However, heterochrony is increasingly being recognized as an important factor in dinosaur evolution. In order to quantitatively analyse the impact of heterochrony on saurischian skull shape, we analysed five ontogenetic trajectories using two-dimensional geometric morphometrics in a phylogenetic framework. This allowed for the comparative investigation of main ontogenetic shape changes and the evaluation of how heterochrony affected skull shape through both ontogenetic and phylogenetic trajectories. Using principal component analyses and multivariate regressions, it was possible to quantify different ontogenetic trajectories and evaluate them for evidence of heterochronic events allowing testing of previous hypotheses on cranial heterochrony in saurischians. We found that the skull shape of the hypothetical ancestor of Saurischia likely led to basal Sauropodomorpha through paedomorphosis, and to basal Theropoda mainly through peramorphosis. Paedomorphosis then led from Orionides to Avetheropoda, indicating that the paedomorphic trend previously found in advanced coelurosaurs may extend back into the early evolution of Avetheropoda. Not only are changes in saurischian skull shape complex due to the large number of factors that affected it, but

47 heterochrony itself is complex, with a number of possible reversals throughout non-avian
48 saurischian evolution. In general, the sampling of complete ontogenetic trajectories including
49 early juveniles is considerably lower than the sampling of single adult or subadult individuals,
50 which is a major impediment to the study of heterochrony on non-avian dinosaurs. Thus, the
51 current work represents an exploratory analysis. To better understand the cranial ontogeny and
52 the impact of heterochrony on skull evolution in saurischians, the data set that we present here
53 must be expanded and complemented with further sampling from future fossil discoveries,
54 especially of juvenile individuals.
55

56 **Introduction**

57 In an evolutionary context, heterochrony describes phenotypic changes due to shifts in the timing
58 or rate of developmental processes in an organism relative to its ancestor, and can lead to
59 significant evolutionary changes in body plans within relatively short periods of time (Gould,
60 1977; Alberch *et al.*, 1979; McNamara, 1982; Reilly, Wiley & Meinhardt, 1997; Klingenberg,
61 1998; McNamara & McKinney, 2005). Two major types of heterochronic processes are
62 discerned: paedomorphosis and peramorphosis. Paedomorphosis occurs when the later
63 ontogenetic stages of an organism retain characteristics from earlier ontogenetic stages of its
64 ancestor due to a truncation of the growth period (progenesis), decrease of the growth rate
65 (neoteny) or a delayed onset of developmental processes (postdisplacement). In contrast, a
66 peramorphic organism is ontogenetically more developed than the later ontogenetic stages of its
67 ancestor due to the extension of growth period (hypermorphosis), the increase of the growth rate
68 (acceleration) or the earlier onset of developmental processes (predisplacement) (see Gould,
69 1977; Alberch *et al.*, 1979; Klingenberg, 1998). In practice, evidence for heterochronic events in

70 evolution can be detected by comparing the ontogenetic trajectories of different taxa under the
71 consideration of their phylogenetic interrelationships (Alberch *et al.*, 1979; Fink, 1982). Thus,
72 the concept of heterochrony connects two main fields of biological sciences: developmental and
73 evolutionary biology (Gould, 1977; Raff, 1996). When studying heterochrony, ontogenetic
74 trajectories are characterized by three separate vectors (size, shape, and ontogenetic age), which
75 allows for quantification of heterochronic processes with slope, length and position within a
76 Euclidean space (Alberch *et al.*, 1979). In this context, geometric morphometrics is a useful
77 method for characterizing shape and size vectors to investigate heterochrony in organisms within
78 a multivariate framework (Mitteroecker, Gunz & Bookstein, 2005).
79
80 Documentation of heterochrony in the vertebrate fossil record is limited. Preserved fossil
81 ontogenetic series covering the whole postnatal development of fossil species are rare due to the
82 fact that early juvenile specimens are often either lacking or incomplete. Furthermore, exact ages
83 of single ontogenetic stages are often not available, resulting in the temporal component often
84 being replaced by size, which is not an ideal variable for age (Klingenberg, 1998; Gould, 2000).
85 Nevertheless, the role of heterochrony has been recognized and discussed for the evolution of
86 multiple fossil lineages that do preserve ontogenetic series (Balanoff & Rowe, 2007; Gerber,
87 Neige & Eble, 2007; Schoch, 2009, 2010, 2014; Bhullar, 2012; Forasiepi & Sánchez-Villagra,
88 2014; Ezcurra & Butler, 2015), including non-avian dinosaurs (e.g. Long & McNamara, 1997;
89 Erickson *et al.*, 2004; Guenther, 2009; Bhullar *et al.*, 2012; Canale *et al.*, 2014). For example,
90 Long & McNamara (1997), Erickson *et al.* (2004) and Canale *et al.* (2014) hypothesized that the
91 evolution of large body size in carcharodontosaurids and tyrannosaurids from medium-sized
92 ancestors was the result of peramorphosis.

93

94 There has recently been an increasing interest in shape diversity in non-avian dinosaurs, in which
95 geometric morphometric methods have been applied on a regular basis (e.g. Bonnan, 2004;
96 Chinnery, 2004; Campione & Evans, 2011; Hedrick & Dodson, 2013; Lautenschlager, 2014;
97 Schwarz-Wings & Böhm, 2014; Maiorino *et al.*, 2015). Skull shape diversity in saurischian
98 dinosaurs has been studied in particular detail (e.g. Henderson, 2002; Young & Larvan, 2010;
99 Rauhut *et al.*, 2011; Brusatte *et al.*, 2012; Bhullar *et al.*, 2012; Foth & Rauhut, 2013a,b), but
100 usually in relation to functional constraints, dietary preferences, phylogenetic interrelationships,
101 and macroevolutionary patterns. For example, these studies have shown that skull shape in
102 sauropodomorphs and theropods is phylogenetic constrained (Young & Larvan, 2010; Brusatte *et*
103 *al*., 2012; Foth & Rauhut, 2013a) and that the shape of the orbit in theropods is functionally
104 constrained (Henderson, 2002; Foth & Rauhut, 2013a). Thus, geometric morphometrics is a
105 powerful method to quantify both intraspecific (e.g. ontogeny, sexual dimorphism,
106 polymorphism) and interspecific (e.g. systematics, macroevolution) shape variation on the basis
107 of homologous landmarks or outlines, which capture more information about shape than
108 traditional morphometric measurements (Corti, 1993; Rohlf & Marcus, 1993; Adams, Rohlf &
109 Slice, 2004, 2013; Slice, 2007; Mitteroecker & Gunz, 2009; Zelditch, Swiderski & Sheets, 2012).
110 As a result, geometric morphometrics has also been successfully applied to the study of
111 heterochrony among various tetrapod groups, in which the univariate mathematical approach of
112 Alberch *et al.* (1979) was adapted to a multivariate framework (e.g. Berge & Pennin, 2004;
113 Mitteroecker *et al.*, 2004; Mitteroecker, Gunz & Bookstein, 2005; Liebermann *et al.*, 2007;
114 Drake, 2011; Piras *et al.*, 2011; Bhullar *et al.*, 2012). However, only Bhullar *et al.* (2012) have
115 examined cranial shape diversity of theropod dinosaurs using multivariate methods in the context

of heterochrony. This pioneering study demonstrated that recent birds have highly paedomorphic skulls compared to non-avian theropods and Mesozoic birds (e.g. *Archaeopteryx* and Enantiornithes), which evolved in a multistep transformation within the clade Eumaniraptora. Furthermore, Bhullar et al. (2012) found evidence for independent peramorphic trends in the skull shape of large-bodied tyrannosaurids, dromaeosaurids and troodontids and proposed a similar trend for allosaurids. Finally, Bhullar *et al*. (2012) hypothesized a possible paedomorphosis for *Eoraptor* and basal sauropodomorphs.

The aim of the current study is to investigate the cranial shape diversity of saurischian dinosaurs by comparing the ontogenetic trajectories of different taxa from both qualitative and quantitative data, using two-dimensional geometric morphometrics (2D GM). This study expands on the work of Bhullar *et al.* (2012) who focused primarily on trends within Maniraptora, derived non-avian theropods and basal avian theropods. We have built upon their study by including an improved sample of basal saurischians and theropods (including a number of different ontogenetic series), which should be more sensitive for testing of the heterochronic changes for allosaurids and basal sauropodomorphs proposed, but not verified statistically, by Bhullar *et al*. (2012). The phylogenetic relationships of the ontogenetic series sampled in this study are integrated into an ancestor-descendant framework to look for further potential heterochronic processes in the cranial evolution of saurischians. However, due to the limited number of ontogenetic series known for sauropodomorphs, the current study focuses primarily on the early evolution of theropods. Nevertheless, due to the limited number of ontogenetic series currently available in our taxonomic sample, this work must be viewed as an exploratory study, which will need to be expanded and complemented with further sampling from future fossil discoveries.

Materials and Methods

Institutional Abbreviations

BMMS, Bürgermeister Müller Museum Solnhofen, Solnhofen, Germany; **CM**, Carnegie Museum of Natural History, Pittsburgh, USA; **GR**, Ruth Hall Museum, Ghost Ranch, USA; **IVPP**, Institute of Vertebrate Paleontology and Paleoanthropology, Beijing, China, **MCZ**, Museum of Comparative Zoology, Harvard University, USA.

Taxon sampling

We sampled the crania of 35 saurischian dinosaur taxa (10 sauropodomorphs and 25 non-pennaraptoran theropods, see Table S3 in the Supplementary Information) on the basis of published reconstructions of adult (or advanced subadult) individuals in lateral view (with exception of the reconstructions of the basal tyrannosauroid *Dilong* [IVPP V14243] and the basal alvarezsauroid *Haplocheirus* [IVPP V15988], which were based on our personal observations). The data set shows an overlap of 15 terminal taxa with that of Bhullar *et al*. (2012) and builds on that study with an addition of 20 new taxa. Theropods with large nasal crests (e.g. *Ceratosaurus*, *Dilophosaurus*, *Guanlong*) were excluded from the primary data set as they were found to have a strong impact on the ancestral shape reconstruction (see below) of Averostra, Avetheropoda, Coelurosauria and Tyrannosauroidea (see Fig. S5, Table S6 in the Supplementary Information). Although cranial crests are a common structure among theropod dinosaurs (Molnar, 2005), reconstruction of moderately to strongly crested hypothetical ancestors within this study would necessarily be artificial due to the lack of intermediate crested forms and relatively small sample size of the available data set. Only *Monolophosaurus* was included in the main data set because

it possesses a rather moderately sized and simple nasal crest. '*Syntarsus' kayentakatae*, which is often reconstructed with a pair of prominent nasal crests (Rowe, 1989; Tykoski, 1998), was analysed in this study without crests since this structure is probably artificial due to post-mortem displacement of the nasals (Ezcurra & Novas, 2005, 2007). As cranial crests usually represent external visual signal structures (Sampson, 1999; Padian & Horner, 2011; Hone, Naish & Cuthill, 2012), their evolutionary development most likely represents either an evolutionary novelty or was sourced from regional peramorphic processes if the primordia were already present in the ancestor (see discussion on the evolution of horns and frills in Ceratopsia by Long & McNamara 1997). However, we generated a second data set that includes crested taxa for comparison with the main data set (see below).

In our sample, five taxa preserve early ontogenetic stages allowing the capture of both juvenile and adult skull shapes, which were used to reconstruct five simplified ontogenetic series, containing two stages (i.e. an early juvenile and adult stage). This sample includes the basal sauropodomorph *Massospondylus*, the basal theropod *Coelophysis*, the megalosaurid *Dubreuillosaurus*, the allosauroid *Allosaurus*, and the tyrannosaurid *Tarbosaurus* (see Table S4 in the Supplementary Information). Two of the ontogenetic series sampled (*Coelophysis* and *Tyrannosaurus*/*Tarbosaurus*) overlap with the data set from Bhullar *et al*. (2012), but we expand on the previous study by including three more basal trajectories in order to concentrate on a different part of the theropod tree. As the fossil record of juvenile dinosaur specimens with complete skull material is rare, the number of ontogenetic series is limited. To improve sampling, previous studies have included reconstructions from multiple partial juvenile skulls or juveniles from closely related taxa (e.g. Bhullar *et al.*, 2012). We implemented this approach in

two cases: the reconstruction of the juvenile *Coelophysis* sample was based on three incomplete, somewhat taphonomically deformed individuals (MCZ 4326; GR 392; CM 31375); and the holotype of *Sciurumimus* (BMMS BK 11) was used as the juvenile representative of the megalosaurid *Dubreuillosaurus* based on the phylogenetic analyses of Rauhut *et al.* (2012). In contrast to Bhullar *et al.* (2012), we did not include the ontogenetic series of *Byronosaurus*, Therizinosauridae (represented by a therizinosaurid embryo and the skull of *Erlikosaurus*) and *Compsognathus* (with the juvenile specimen represented by *Scipionyx*) in the data set because the postorbital region of the juvenile skulls of the former two taxa is crushed or incomplete (Bever & Norell, 2009; Kundrát *et al.*, 2009), and the taxonomic referral of *Scipionyx* to the clade Compsognathidae (see Dal Sasso & Maganuco, 2011) is uncertain and maybe an artefact of coding juvenile character states (see Rauhut *et al.*, 2012).

Two-dimensional Geometric Morphometrics (2D GM)

We used 20 landmarks (LMs) and 51 semi-landmarks (semi-LMs) on our sample in order to accurately capture skull shape. The landmarks were collected using the software tpsDig2 (Rohlf, 2005) and were classified as either type 1 (points where two bone sutures meet) or type 2 (points of maximum curvature and extremities) (Bookstein, 1991) (see Fig. S1, Table S1 in the Supplementary Information for full description). Type 3 landmarks (points constructed between two homologous landmarks, which mainly define the shape of the skull or skull openings rather than the position of exact homologous points) were not used in our study. Semi-landmarks were used to capture the shape of skull openings and the skull outline by defining a number of points that are placed equidistantly along respective curves (Bookstein, 1991; Bookstein *et al.*, 1999). The percent error for digitizing each landmark and semi-landmark was estimated for the skull

208 reconstruction of the juvenile *Coelophysis* (with n = 10 replications) using the method described
209 by Singleton (2002). Landmark and semi-landmark error varies between 0.117 percent (LM 51 -
210 most posterior point of the descending process of the maxilla contacting the nasal and/or the
211 lacrimal) and 0.738 percent (LM 3 - contact between the maxilla and jugal along the ventral
212 margin of the skull) with a mean of 0.283 percent. The error has no significant effect on the
213 shape analyses (see Table S2 in the Supplementary Information).
214
215 The shape coordinates were then imported into the software package MorphoJ 1.05d
216 (Klingenberg, 2011) and superimposed using generalized Procrustes analysis (GPA). GPA
217 rotates, translates and resizes landmark coordinates of all specimens accounting for all non-shape
218 related differences between landmark configurations, leaving only shape information (Gower,
219 1975; Rohlf & Slice, 1990). Although semi-landmarks have fewer degrees of freedom than
220 regular landmarks (and thus contain less shape information) (Bookstein, 1991), we treated
221 landmarks and semi-landmarks as equivalent for GPA (Zelditch, Swiderski & Sheets, 2012) and
222 did not slide the semi-landmarks. The sliding process created considerable artificial deformation
223 on the Procrustes-fitted shape in some taxa (see Fig. S2 in the Supplementary Information).
224 However, due to the equivalent weighting of landmarks and semi-landmarks, it should be kept in
225 mind that the shape information captured by the semi-landmarks strongly influences the results
226 (Zelditch, Swiderski & Sheets, 2012; see below). In order to estimate the influence of the semi-
227 landmarks on the shape data, all analyses described below were also applied to an additional data
228 set that included only landmark data (see Supplementary Information).
229

The generated Procrustes coordinates were used to compare juvenile and adult skull shapes to each other in each ontogenetic series to find ontogenetic patterns between and within taxa. Furthermore, the Procrustes coordinates of all taxa (including juvenile specimens) were subjected to an exploratory principal components analysis (PCA) using the covariance matrix generated from Procrustes coordinates. PCA simplifies descriptions of variation among individuals by creating new sets of variables that are linear combinations of the original set such that the new sets are independent from one another and have zero covariance. The principal components (PCs) describe successively smaller amounts of total variance of the sample. This allows for a larger proportion of the variance to be described using a smaller number of variables than the original data would have allowed (Zelditch, Swiderski & Sheets, 2012). A multivariate regression of the Procrustes coordinates against log-transformed centroid sizes (= square root of the sum of the squared distances of each landmark to the centroid of the landmark configuration, Zelditch, Swiderski & Sheets, 2012) was performed to test if the skull shape variation is correlated with size and contains allometric information (Drake & Klingenberg, 2008).

Quantification of ontogenetic trajectories

The different ontogenetic trajectories generated in the PCA and regression analyses were compared to each other by calculating pairwise two-dimensional angles between different trajectories based on the PC values of the first three axes, which are the significant principal components (significance calculated using the broken stick method, see Jackson, 1993). Each of the two-stage ontogenetic trajectories was described as a phenotypic change vector, $\Delta \vec{y}_i = \vec{y}_{ij} - \vec{y}_{ik}$, with two shape traits (PC 1 vs. PC 2 and PC 1 vs. PC 3), where *i* is a specific ontogeny between two fixed stages, juvenile (*j)* and adult (*k)* (Collyer & Adam, 2007). The difference in direction

(angle) between the ontogenetic phenotypic change vectors $\Delta \vec{y}_a, \Delta \vec{y}_b$ was calculated using the dot product $\cos^{-1}(\Delta \vec{y}_a, \Delta \vec{y}_b) = \frac{\Delta \vec{y}_a \cdot \Delta \vec{y}_b}{|\Delta \vec{y}_a||\Delta \vec{y}_b|}$. PC values were employed to calculate the length of each ontogenetic trajectory. Lengths and angles were used to characterise the differences between the ontogenetic trajectories in relation to shape variation.

Phylogenetic framework for heterochronic analyses

In an evolutionary context, heterochrony is defined as the change in the timing or rate of developmental processes in ancestor-descendant relationships (Alberch *et al*., 1979; Fink, 1982; Klingenberg, 1998), and thus a direct comparison of ontogenetic trajectories from different species (as terminal taxa) can be problematic because it is hard to determine which trajectory would represent the ancestral and the descendant form, respectively (see Fink 1982). This is exacerbated when the supposed ancestral (terminal) species possesses an unknown, long evolutionary history resulting from a ghost lineage. This problem can be partially solved using a phylogenetic approach (see Alberch *et al*., 1979; Fink 1982; Balanoff & Rowe. 2007; Bhullar, 2012; Fritsch, Bininda-Emonds & Richter, 2013; Mallon *et al*., 2015), in which the ancestor of two sister (terminal) taxa is represented by the hypothetical last common ancestor (Hennig, 1966). Therefore, on the basis of the phylogenetic distribution of the five ontogenetic series sampled we calculated hypothetical ancestral ontogenetic trajectories for Saurischia, Neotheropoda, Orionides and Avetheropoda using ancestral shape reconstructions as follows (see Fig. S3, S4 in the Supplementary Information). An informal supertree (sensu Butler & Goswami, 2008) including all taxa with adult individuals was created based on recent phylogenetic analyses (see Fig. S3, S4 in the Supplementary Information): basal

Sauropodomorpha (Cabreira *et al*., 2011), Coelophysoidea (Ezcurra & Novas, 2007), Ceratosauria (Pol & Rauhut, 2012), Tetanurae (Carrano, Benson & Sampson, 2012), and Coelurosauria (Turner *et al.*, 2012; Loewen *et al*., 2013). The phylogenetic position of *Eoraptor* follows Martínez *et al.* (2011) and Martínez, Apaldetti & Abelin (2013). The position of *Adeopapposaurus* as sister taxon of *Massospondylus* follows Martínez (2009). The position of *Herrerasaurus* and *Tawa* at the base of Theropoda is based on Sues *et al*. (2011). *Zupaysaurus* was placed outside Coelophysoidea as one of the successive sister taxa of Averostra (Smith *et al.*, 2007; Sues *et al*., 2011; Ezcurra, 2012). The supertree was time-calibrated using the stratigraphic age of each taxon (as mean of time interval) (see Table S3, S5 in the Supplementary Information). The assignment of branch lengths was performed in R (R Development Core Team, 2011) using the APE package (version 2.7-2; Paradis, Claude & Strimmer, 2004) and a protocol written by Graeme Lloyd (see http://www.graemetlloyd.com/methdpf.html) for adjusting zero branch lengths by sharing out the time equally between branches (see Brusatte *et al*., 2008; Brusatte, 2011), and adding an arbitrary length of 1 million years to the root. The time-calibrated supertree was imported into the software package Mesquite 2.72 (Maddison & Maddison, 2009). Subsequently, Procrustes coordinates and centroid sizes of the adult representatives of the taxa were mapped onto the supertree as continuous characters using square change parsimony. This algorithm performs an ancestral state reconstruction by collating the sum of squared changes of continuous characters along all branches of a tree and estimates the most parsimonious ancestral states by minimizing the total sum of squared changes across the tree (Maddison, 1991). In the next step we tested if the continuous data contains a phylogenetic signal. We performed a permutation test in MorphoJ in which the topology was held constant and both the Procrustes-fitted shape data and the centroid size for each taxon were randomly

298 permuted for all the terminals across the tree 10,000 times (Laurin, 2004; Klingenberg &
299 Gidaszewski, 2010). The data are considered to contain a statistically significant phylogenetic
300 signal if the squared length of the original supertree occurs in at least 95% of the randomly
301 generated trees. Additionally, we quantified phylogenetic signal in our data using a multivariate
302 form of the *K* statistic with 10,000 replications (Blomberg *et al.*, 2003; Paradis, 2012; Adams,
303 2014) in R using the package geomorph (Adams & Otárola-Castillo, 2013). This test estimates
304 the strength of a phylogenetic signal in a data set in relation to a simulated Brownian motion
305 model, which is expressed as *K* and *p* values.
306
307 To obtain ancestral ontogenetic trajectories, the protocol described above was repeated in a new
308 nexus file containing the Procrustes-fitted shapes and centroid sizes of the juvenile specimens.
309 As the juvenile data set is only represented by five taxa, the original supertree was pruned such
310 that only these taxa remained, retaining the original time-calibration. Finally, the ancestral
311 Procrustes-fitted shapes and centroid sizes of both juvenile and adult Saurischia, Neotheropoda,
312 Orionides and Avetheropoda were exported and combined with the respective data from the
313 ontogenetic trajectories of the terminal taxa. The ancestral Procrustes-fitted shape of Averostra
314 was not considered because no ceratosaur juveniles have been published in detail so far (see
315 Madsen & Welles, 2000). The new data set including the five terminal and four ancestral
316 ontogenetic trajectories was loaded again into MorphoJ.
317
318 **Regression analyses of ontogenetic trajectories**
319 A multivariate, pooled within-group regression of shape against log-transformed centroid size
320 including terminal taxa and hypothetical ancestors (see above) was performed (Piras *et al*., 2011;

Bhullar et al., 2012; Zelditch, Swiderski & Sheets, 2012), in which the Procrustes coordinates were transformed into a regression score (see Drake & Klingenberg, 2008). In contrast to many previous studies of heterochrony using geometric morphometrics, which compare only the ontogenetic trajectories of terminal taxa, our approach allows the determination of possible heterochronic patterns between ancestors and descendants. The different ontogenetic trajectories were compared regarding slope, length, angles and range of shape variation spanned by the predicted regression score. The angles between ontogenetic trajectories were calculated based on Procrustes distances and centroid sizes (see above).

As mentioned above, studies of heterochrony require size, shape and ontogenetic age as independent vectors (Klingenberg, 1998). Due to missing data on the individual age of the specimens, ontogenetic age could not be taken into account. As a consequence, the regression analysis explores allometry and not heterochrony (Klingenberg & Spence, 1993; Klingenberg, 1998; Gould, 2000). While some heterochronic processes can result from allometric changes (e.g. acceleration and neoteny), allometric studies allow only conclusions regarding paedomorphosis and peramorphosis (Klingenberg & Spence, 1993; Klingenberg, 1998), which are expressed by the shape vector (i.e. regression score). Peramorphosis can be inferred if the adult individual of the descendant trajectory falls along higher regression scores than the respective ancestral one, whereas paedomorphosis can be inferred based along lower scores. To verify the results of such regression analyses we repeated the analysis using Euclidean distance, which is equivalent to Procrustes distance (see Singleton, 2002; Tallman *et al*., 2013) as a separate shape vector measuring differences in shape. The Euclidean distance matrix was calculated in PAST 3.05 (Hammer, Harper & Ryan, 2001) on the basis of the Procrustes

coordinates of terminal taxa and hypothetical ancestors (see above), which were exported from MorphoJ. For regression analysis, the juvenile specimen of *Massospondylus*, which represents the sample with the smallest centroid size, was set to zero for aligning the distance values of the remaining taxa (Fig. 4).

To test if the shape changes, and as a result the presence of heterochrony, of an ancestor-descendant relationship are statistically meaningful, we calculated the confidence interval (CI) of the differences between regression scores and Euclidean distances of terminal and ancestral taxa (n = 68) and compared them with the differences of ancestral and descendant regression scores from the sub-sample containing the ontogenetic trajectories. Changes were considered significant if the differences between regression scores were at least 1.5 times higher than the CI value (see Cumming, Fidler & Vaux, 2007).

For comparison, we performed another PCA with the data set containing just terminal and ancestral ontogenetic trajectories and calculated the angles and lengths of the trajectories on the basis of the first two principal components, which were found to contain all significant shape information based on the broken stick method (see above).

Finally, the ancestral shape reconstructions calculated for the adult representatives of the taxa were used to qualitatively discuss the evolutionary changes within basal Sauropodomorpha and Theropoda with respect to the ontogenetic changes and heterochronic trends found in the different trajectories.

Results

General ontogenetic changes

The juveniles of the sauropodomorph *Massospondylus* and the theropods that were sampled here tend to have skulls with a short and abruptly tapering snout, short antorbital fenestrae, large subcircular orbits, slender jugals, and dorsoventrally deep orbital and postorbital regions relative to the snout. In addition, the jaw joint is more anteriorly placed relative to the occiput, with exception of the juvenile specimen of *Allosaurus* sampled here. The general ontogenetic pattern includes an elongated and dorsoventrally deeper snout relative to the orbital and postorbital regions, and also a relative increase in size of the antorbital fenestra, which correlates with a relative decrease in size of the orbit. Finally, the jugal becomes more massive in all taxa, which is more pronounced in the large-bodied theropods *Allosaurus* and *Tarbosaurus* (Fig. 1). The relative elongation of the snout and antorbital fenestra were not observed in the *Allosaurus* or *Tarbosaurus* ontogenies, which is probably due to the fact that the juveniles sampled do not represent the earliest ontogenetic stages (Loewen, 2009; Tsuihiji *et al.*, 2011, see discussion). However, the discovery of an isolated maxilla identified as a hatchling allosauroid might indicate that the snout of early *Allosaurus* juveniles was probably short and subsequently increased in relative length during early ontogeny (Rauhut & Fechner, 2005).

In addition to these more general ontogenetic modifications, individual taxa show specific shape changes (Fig. 1):

a) In *Massospondylus* the external naris becomes larger and expands dorsally. The postorbital also becomes relatively more robust. The infratemporal fenestra decreases in relative size. The jaw joint moves anteroventrally.

b) In *Coelophysis* the external naris becomes smaller and shifts anteriorly. The notch of the alveolar margin between the premaxilla and maxilla decreases in relative size during ontogeny, while the alveolar margin of the premaxilla becomes more aligned with that of the maxilla. The descending process of the lacrimal becomes more slender anteroposteriorly. The postorbital becomes more gracile in its relative shape. The infratemporal fenestra increases in relative size. The jaw joint moves posterodorsally.

c) In the megalosaurid taxon, the external naris becomes relatively larger and expands posteriorly. The lacrimal is inclined strongly backwards and the postorbital becomes relatively more robust. The infratemporal fenestra increases in its relative size. The jaw joint moves posteriorly.

d) In *Allosaurus* the external naris does not change in relative size, but shifts ventrally. The descending process of the lacrimal becomes more massive anteroposteriorly. The lacrimal develops a prominent dorsal horn through ontogeny. In contrast to previous taxa, the postorbital region of *Allosaurus* increases dorsoventrally such that the postorbital, quadratojugal and squamosal become relatively more robust. The ventral shift of the jugal leads to the formation of a wide angle between the ventral margins of the maxilla and jugal. Due to its posteroventral expansion, the postorbital affects the shape of the infratemporal fenestra. However, the infratemporal fenestra does not decrease in its relative size, but shifts anteroventrally. The jaw joint moves anteroventrally.

e) In *Tarbosaurus* the external naris does not change in relative size, but shifts dorsally. As in *Allosaurus*, the descending process of the lacrimal becomes more massive. The same is true for the postorbital region, which increases in depth dorsoventrally. This change is

correlated with the development of a more robust postorbital, quadratojugal and squamosal. The jaw joint moves posteroventrally.

Principal component analysis and phylogenetic correlation

The first three principal components account for 68.0% of the total variation (PC 1: 30.8 %; PC 2: 23.9 %; PC 3: 13.3 %), in which PC 2 and PC 3 contain the main allometric shape information (see Table S12 in the Supplementary Information). PC 1 describes the overall skull depth, size and anteroposterior position of the external naris, length of the premaxilla, size of the maxillary antorbital fossa, and position of the lacrimal and postorbital on the anteroposterior axis (affecting the size of the antorbital fenestra, orbit and infratemporal fenestra). The dorsoventral dimension of the orbit is affected by the relative depth of the entire orbital and postorbital regions, while that of the infratemporal fenestra is affected by the relative position of the jugal-quadratojugal bar. The variation in the depth of the skull also affects the position of the jaw joint on the dorsoventral axis (Fig. 2c). PC 2 describes the length of the snout caused by variation in the length of the maxilla and inclination and anteroposterior position of the lacrimal. The inclination of the lacrimal affects the size of the antorbital fenestra, while both position and inclination affect the anteroposterior dimension of the orbit. PC 2 also accounts for the length and the dorsoventral position of the external naris and size of the upper temporal region (Fig. 2c). PC 3 describes the length of the premaxilla, posterior extension of the external naris, dorsoventral height of the maxilla, and anteroposterior dimension of the ventral process of the lacrimal (which affects the shape of the antorbital fenestra and orbit). The shape of the orbit is further affected by the anteroposterior dimension of the jugal-postorbital bar. Further variation captured by PC 3 is related to the shape of the skull roof in the orbital and postorbital regions, dorsoventral height of

435 the infratemporal fenestra, and position of the jaw joint on the anterodorsal-posteroventral axis
436 (Fig. 2c).
437
438 The permutation tests and the multivariate *K* statistic recovered that both Procrustes-fitted shapes
439 (tree length weighted by branch lengths = 0.5108, $p < 0.0001$; $K = 0.2607$, $p = 0.0016$) and
440 centroid size (tree length weighted by branch lengths = 8.3598, p = 0.0005; $K = 0.8900$, $p =$
441 0.0002) are correlated with phylogeny. Furthermore, the multivariate regression analysis reveals
442 that skull shape is significantly correlated with centroid size (correlation index: 15.32%, p
443 <0.0001) (Fig. 4a, Table S12 in the supplementary Information).
444
445 **Ontogenetic trajectories in the PCA morphospace**
446 Based on the PCA results of the original data set (i.e. including semi-landmarks), the ontogenetic
447 trajectories are not uniform (Fig. 2, Table 1). The trajectory of *Allosaurus* is short and mainly
448 explained by shape variation captured by PC 1, while that of *Tarbosaurus* is also short, but
449 mainly explained by PCs 1 and 3. The third principal component has stronger influence on the
450 ontogenetic shape variation in *Tarbosaurus* based on the length of its trajectory. Compared to
451 *Allosaurus* and *Tarbosaurus*, the other ontogenetic trajectories are longer. The trajectory of
452 *Coelophysis* is mainly explained by the shape variation captured by PCs 1 and 2, while its slope
453 is opposite to the direction along PC 1 compared to the trajectories of *Allosaurus* and
454 *Tarbosaurus*. Based on the angles, the ontogenetic trajectories of *Massospondylus* and the
455 megalosaurid taxon are mainly influenced by the shape variation captured by PCs 2 and 3, in
456 which the ontogenetic trajectory of *Massospondylus* is directed in the opposite direction along
457 PC 3 to that of the megalosaurid taxon and *Tarbosaurus*. However, the length of the trajectories

458 indicates that the second principal component has major influence on the shape variation in both
459 species during ontogeny.
460
461 The PCA reveals that the ontogenetic elongation of the snout is primarily related to a relative
462 increase in the length of the maxilla (PCs 1, 2). In *Massospondylus* and the megalosaurid taxon
463 the ontogenetic elongation of the snout is further affected by the relative increase of the length of
464 the premaxilla (PC 3). The relative increase in snout depth results mainly from a ventral
465 expansion of the maxilla, which is more prominent in *Allosaurus* and *Tarbosaurus* than in other
466 taxa (PCs 1, 3). In the megalosaurid taxon and *Allosaurus,* maxillary deepening occurs together
467 with a dorsoventral expansion of the nasal (PC 1). Additionally, dorsoventral expansion of the
468 premaxilla is observed in *Allosaurus* and *Tarbosaurus* (PC 1). The relative elongation of the
469 snout in *Massospondylus*, the megalosaurid taxon and *Coelophysis* correlates with a relative
470 increase in the anteroposterior length of the antorbital fenestra, caused by a posterior shift of the
471 lacrimal and elongation of the maxilla (PCs 1, 2). Additionally, in *Coelophysis* the anterior
472 border of the antorbital fenestra extends anteriorly (PC 1). In both *Massospondylus* and the
473 megalosaurid taxon, the antorbital fenestra is shifted posteriorly during ontogeny (PC 2). The
474 megalosaurid taxon shows a further dorsal expansion of the antorbital fenestra (PC 3), not seen
475 in the latter two taxa. Although no relative size changes could be observed in the antorbital
476 fenestrae of *Allosaurus* and *Tarbosaurus*, the antorbital fenestra of *Allosaurus* shifts
477 posterodorsally during ontogeny, whereas that of *Tarbosaurus* shifts ventrally. In most
478 trajectories, the most anterior point of the antorbital fossa shifts posteriorly during ontogeny (PCs
479 1−3), but a relative decrease in the length of the maxillary antorbital fossa is present in
480 *Allosaurus* and *Tarbosaurus* (PC 1). In the megalosaurid taxon, the anterior margin of the

antorbital fossa shifts ventrally, whereas in *Coelophysis* it shifts anteriorly (PC 1), which correlates with the anterior elongation of the antorbital fenestra in this taxon (see above). As mentioned above, the orbit decreases in relative size in all taxa during ontogeny (PCs 1−3). In *Coelophysis* and *Massospondylus* this is related to a relative shift of the lacrimal posteriorly (PCs 1, 2). In the megalosaurid taxon, *Allosaurus* and *Tarbosaurus* the relative size reduction is correlated with a change in orbital shape from subcircular to oval. In the megalosaurid taxon these changes are linked to a posterior shift of the lacrimal (PC 2) and anterior shift of the postorbital and ascending process of the jugal (PC 3), which is correlated with an anterior extension of the infratemporal fenestra. In *Allosaurus*, the ontogenetic changes of the orbit are related to the posterior extension of the lacrimal and anterior shift of the postorbital and ascending process of the jugal (PC 1). Additionally, the orbit of *Allosaurus* is shifted slightly dorsally. In *Tarbosaurus*, these changes result from an anterior extension of both the postorbital and ascending process of the jugal (PC 3). The orbit of *Tarbosaurus* becomes posteriorly constricted by an anterior shift of the ventral process of the postorbital, forming a suborbital process.

We examined the differences in the trajectory directions when terminal and ancestral ontogenetic series are compared to each other (Fig. 3, Table 2). The significant shape variation evaluated via the broken stick method is described by the first two principal components (PC1: 50.39 %; PC2: 20.79 %). Both axes are correlated with centroid size (see Table S12, Supplementary Information). The ontogenetic trajectory of *Coelophysis* in mainly influenced by PC 1, while that of the megalosaurid taxon, *Massospondylus* and all ancestral trajectories is influenced by both PC 1 and 2, in which the first principal component is found to have a higher impact on the shape

variation during ontogeny. In contrast, the ontogenetic trajectories of *Tarbosaurus* and *Allosaurus* are mainly influenced by PC2.

Ontogenetic trajectories in the regression analyses

The ontogenetic trajectory of *Massospondylus* is longer than that of the hypothetical ancestor of Saurischia for both shape variables (regression score and Euclidean distance), while the values of the shape variables are significantly lower. However, the slope of the trajectory of *Massospondylus* based on the regression score is less pronounced than that of the saurischian ancestor, while it is more pronounced for the Euclidean distance (Fig. 4b, c, Table 3, 4). In contrast, the ontogenetic trajectory of the hypothetical ancestor of Neotheropoda is slightly longer and has a greater slope, while the regression score and the Euclidean distance of the adult individual are significantly higher than that of the saurischian ancestor. *Coelophysis* possesses a longer and steeper ontogenetic trajectory for both shape variables with significantly higher values than the hypothetical ancestor of Neotheropoda (Fig. 4b, c, Table 3, 4). The ontogenetic trajectory of the hypothetical ancestor of Orionides is shorter and has a lower slope than that of the neotheropod ancestor. The regression score of the adult individual is significantly higher, while the Euclidean distance is lower, but not significantly different. Compared to the hypothetical ancestor of Orionides, the megalosaurid taxon has a longer and steeper ontogenetic trajectory, with a significantly higher value for both shape variables (Fig. 4b, c, Table 3, 4). In contrast, the ontogenetic trajectory of the hypothetical ancestor of Avetheropoda is shorter, possessing a lower slope and significantly lower regression score and Euclidean distance for the adult individual, when compared to the hypothetical ancestor of Orionides. The ontogenetic trajectories of *Allosaurus* and *Tarbosaurus* are longer than that of the hypothetical ancestor of

Avetheropoda. Both trajectories show a slope decrease compared to their common ancestor. Interestingly, the slope is almost zero when the Euclidean distance is applied as shape variable, indicating only minor shape changes during the ontogeny as sampled. For *Allosaurus*, both shape values of the adult individual are higher than that of the ancestor, but only the regression score is significant. In contrast, the regression score of the adult individual of *Tarbosaurus* is significantly lower than that of the hypothetical ancestor of Avetheropoda, while the Euclidean distance results in a higher, but non statistically significant value (Fig. 4b, c, Table 3, 4).

Based on the regression analysis, taxa with higher regressions scores tend to have elongated skulls with long and slender snouts that have a rounded anterior end, and possess anteroposteriorly long antorbital fenestrae, oval orbits and a post-rostrum only slightly dorsoventrally higher than the snout. The maxilla increases in its relative length, but also expands ventrally. The ascending process of the maxilla, the anterior and ascending processes of the jugal, and postorbital become more massive. In contrast, low regression scores account for skull shapes where these features are less pronounced, developed or even show opposite trends. When compared to the regression analyses containing all taxa, the relative position, length and slopes of the ontogenetic trajectories of the terminal taxa is almost identical (Fig. 4a), supporting the robustness of the results recovered.

Discussion

Ontogenetic patterns

Our knowledge of the cranial ontogeny of non-avian dinosaurs remains fragmentary. Previous studies on cranial ontogeny have often been based on single species (Gow, Kitching & Raath,

1990; Carr & Williamson, 2004; Horner & Goodwin, 2006; Hübner & Rauhut, 2010; Campione & Evans, 2011; Mallon *et al*., 2011; Canale *et al*., 2014; Frederickson &Tumarkin-Deratzian, 2014), while only a small number of studies have investigated this topic on the interspecific level (Carr, 1999; Evans, 2010; Bhullar *et al*., 2012; Mallon *et al*., 2015). As is common in other animal groups, closely related species often undergo similar ontogenetic changes (see Evans, 2010; Mallon *et al*., 2015), while ontogenetic trajectories become more different with increased phylogenetic distance (see Bhullar *et al*., 2012) or in the case of a single taxon evolving extreme ontogenies compared to their relatives (Horner & Goodwin, 2009, see also Erickson *et al*., 2004). Despite the large phylogenetic distance between the ontogenetic series sampled here, the present study reveals that the cranial ontogeny of saurischian dinosaurs undergoes some general patterns, including the relative elongation and dorsoventrally heightening of the preorbital region, decrease in orbit size and increase in jugal robustness. However, the PCA shows that the different ontogenetic trajectories differ strongly in length, direction and also the location within the morphospace. Here, the theropod taxa are markedly separated from the sauropodomorph *Massospondylus*, which is morphologically very distinct from other basal sauropod taxa. This is especially obvious in the large distance within morphospace between *Massospondylus* and *Coelophysis*, which represent the most basal ontogenetic series of each clade indicating a strong diversification of skull shape in the early evolution of Saurischia. This may be related to differentiations along both lines of Saurischia in terms of ecology, including trophic specializations (see Tykoski & Rowe, 2004; Barrett & Rayfield, 2006; Langer *et al*., 2010; Sakamoto, 2010). The fact that the separation within the morphospace already take place among juvenile specimens indicates that these specializations might appear very early in ontogenetic

572 development. Although the distances among such specimens in morphospace are large, the
573 trajectories show that both species still share similar trends in cranial development (Fig. 2, 3).
574
575 Although occupying a similar area of morphospace, the ontogenetic trajectory of the
576 megalosaurid taxon differs markedly from that of *Allosaurus* and *Tarbosaurus*, showing more
577 similarity with that of *Massospondylus* and *Coelophysis*, which share in common the relative
578 elongation of the snout. The latter process probably represents a morphological trend within
579 megalosaurids (Therrien & Henderson, 2007; Sadleir *et al*., 2008), while large-bodied
580 allosauroids and tyrannosaurids tend to have rather deeper than long skulls (see Brusatte *et al*.,
581 2012; Foth & Rauhut, 2013). However, as several medium-sized tyrannosauroids also have
582 elongated snouts (Li et al., 2010; Brusatte, Carr & Norell, 2012; Lü et al., 2014; Porfiri et al.
583 2014), their ontogenetic trajectories would probably more closely resemble that of the
584 megalosaurid taxon. One has to take into account that the length and direction of the ontogenetic
585 trajectories of *Allosaurus* and *Tarbosaurus* are likely influenced by the fact that the juvenile
586 specimens are ontogenetically more developed compared to that of the megalosaurid taxon (see
587 below). Assuming that the hatchlings of *Allosaurus* and *Tarbosaurus* also had short, tapering
588 snouts, the trajectory would probably be more similar in length and direction to that of the
589 megalosaurid taxon.
590
591 **Heterochronic patterns**
592 Previous workers have hypothesized that skull shape diversity in theropods and
593 sauropodomorphs was driven by phylogenetic interrelationships, dietary preferences (Young &
594 Larvan, 2010; Brusatte *et al*., 2012; Foth & Rauhut, 2013a), functional constraints (Henderson,

595 2002; Foth & Rauhut, 2013a), but also heterochrony (Long & McNamara, 1997; Bhullar *et al.*,
596 2012). This study builds on the recent heterochronic analysis of Bhullar et al. (2012), who
597 primarily examined derived non-avian theropods and basal avians on the basis of a great number
598 of ontogenetic trajectories of non-avian coelurosaurs and an extant phylogenetic bracket of
599 crocodylians and birds, covering a broader scale of archosaurian craniofacial shape variation.
600 However, by sampling and comparing ontogenetic trajectories of more basal saurischian taxa,
601 our data set allows for reevaluation of the conclusions presented by Bhullar et al. (2012) with
602 regards to basal sauropodomorphs, allosauroids and tyrannosauroids. The current study supports
603 the influence of heterochrony on the cranial evolution of some saurischian lineages. When the
604 differences of the regressions scores (ΔRS) and the Euclidean distances (ΔED) in an ancestor-
605 descendant relationship are compared, the significant decrease of the shape values indicates
606 potential paedomorphosis for the skull shape of *Massospondylus* and the hypothetical ancestor of
607 Avetheropoda, while the skulls of *Coelophysis*, the megalosaurid taxon and the hypothetical
608 ancestor of Neotheropoda, might be peramorphic. Thus, the current analyses support a
609 paedomorphosis for basal sauropodomorphs as predicted by Bhullar *et al.* (2012). Due to
610 contradicting results regarding shape differences, no heterochronic pattern can be inferred for
611 *Allosaurus*, *Tarbosaurus* and the hypothetical ancestor of Orionides. Thus, the current analyses
612 do not support the predicted cranial peramorphosis for the allosauroids and tyrannosaurid lineage
613 (Long & McNamara, 1997; Bhullar *et al.* 2012; Canale *et al.*, 2014), while studies on growth
614 (Bybee, Lee & Lamm, 2006; Erickson *et al*., 2006) and body size evolution (Dececchi &
615 Larsson, 2013; Benson *et al*., 2014; Lee *et al*., 2014) in theropods indicate such a trend.
616 However, this conflict is probably caused by incomplete sampling of ontogenetic trajectories,
617 which affects the estimated shape of the hypothetical ancestor of Avetheropoda. A further

618 expansion of the sampling of ontogenetic trajectories of saurischian taxa and the inclusion of an
619 extant phylogenetic bracket (see Bhullar *et al.*, 2012), would probably change some aspects of
620 the analytical outcomes of this study (see below).
621
622 The increase in slopes in the ontogenetic trajectories of Neotheropoda, *Coelophysis* and the
623 megalosaurid taxon, when compared to their ancestors, might show evidence for peramorphic
624 acceleration. However, with a few exceptions, bone histology of basal theropods (e.g.
625 *Coelophysis* and *Syntarsus*) is not well studied, so that this cannot be confirmed by growth
626 patterns. Several studies on body size evolution support a peramorphic trend, showing an
627 increase of size from the hypothetical ancestor of Saurischia over Neotheropoda towards
628 megalosaurids (Irmis, 2011; Dececchi & Larsson, 2013). In contrast, the relative decrease in
629 slope in the ontogenetic trajectory of the hypothetical ancestor of Avetheropoda might indicate
630 neoteny. But again this cannot be confirmed by bone histological data at this time. Dececchi &
631 Larsson (2013) and Lee *et al.* (2014) found a decrease of body size from the hypothetical
632 ancestor of Tetanurae towards Avetheropoda, supporting a paedomorphic trend in body size. For
633 *Massospondylus*, the situation is not entirely clear, as our two shape variables led to conflicting
634 results regarding the slope, when compared with the saurischian ancestor. Thus, no underlying
635 heterochronic process can be diagnosed for the paedomorphic skull shape of *Massospondylus*.
636 Although basal sauropodomorphs show a gradual trend towards bigger body size (Sander *et al.*,
637 2010; Irmis, 2011; Benson *et al.*, 2014) and longer, accelerated growth (Chinsamy 1993;
638 Erickson, Rogers & Yerby, 2001; Klein & Sander 2007), skull size decreased relatively (Rauhut
639 et al., 2011). This relative shrinking might be the reason for the maintenance of a more juvenile
640 skull shape in the early evolution of sauropodomorphs. However, due to the lack of information

641 regarding the ontogenetic age of the individuals, the deduction of heterochronic process related
642 to the slope (i.e. neoteny and acceleration) has to be considered with caution (see below).
643
644 The results of the regression analyses can be further used to interpret evolutionary shape changes
645 found between hypothetical ancestors and terminal taxa in the ancestral shape reconstruction
646 analyses of the main sample (i.e. continuous character mapping of the Procrustes-fitted shapes)
647 in terms of paedomorphic or peramorphic trends (Fig. 5). Comparing the skull shape of the
648 hypothetical ancestor of Saurischia to that of Sauropodomorpha indicates a possible initial
649 paedomorphosis in the evolution of the latter group as shown by the regression analyses, which
650 is depicted by a decrease in the relative length of the preorbital region and an increase in the
651 relative orbital size and depth of the postorbital region. As stated above, Bhullar *et al*. (2012)
652 already proposed a cranial paedomorphosis for basal sauropodomorphs after finding a strong
653 similarity between the skull shape of *Eoraptor* and the juvenile theropod *Coelophysis*, which had
654 been also highlighted qualitatively by previous authors (e.g. Ezcurra, 2007). In addition, Foth
655 (2013) has shown that the skull shape of *Eoraptor* and *Pampadromaeus* resembled that of the
656 juvenile theropods *Sciurumimus* and *Juravenator*. In Eusauropoda the snouts become more
657 aberrant due to a dorsal shift of the external naris, posterodorsal extension of the premaxilla,
658 elongation of the ascending process of the maxilla and modification of the postorbital region,
659 affecting the relative size of the jugal and postorbital, which become more gracile (Wilson &
660 Sereno, 1998; Rauhut *et al.*, 2011). While the shape changes in the snout and the shift of the
661 naris were previously presumed to be peramorphic (Long & McNamara, 1997), one can assume
662 on the basis of the current observations that the increase of gracility in the postorbital region of
663 derived sauropods may result from modular paedomorphosis. In this context, Salgado (1999) has

hypothesized that the reduction of the supratemporal fenestra and fusion of the frontals in diplodocoid sauropods is the result of a peramorphic heterochrony, while the loss of contact between squamosal and quadratojugal could be paedomorphic. However, these character changes are beyond the scope of the current study due to the lack of good skull material of juvenile individuals of basal sauropods, and thus, need to be analysed in more detail in future studies after the appropriate juvenile materials are discovered.

In contrast, the initial evolutionary changes in the skull shape of Theropoda were driven by peramorphic events, as is observed in *Coelophysis*, the megalosaurid taxon and the hypothetical ancestor of Neotheropoda in the regression analyses. These changes include the elongation of the snout, increase in length of the antorbital fenestra, and trends to a relatively smaller orbit and more robust post-rostral region. The basal ceratosaur *Limusaurus* has a rather small skull with a short snout, enlarged subcircular orbit and gracile jugal and postorbital, so it is possible that the more robust skull shape (oval orbit, massive jugal and postorbital) of large-bodied ceratosaurs like *Ceratosaurus* and abelisaurids (e.g. *Carnotaurus* and *Majungasaurus*) could be the result of a secondary peramorphosis as it was proposed for allosaurids and tyrannosaurids (e.g. Long & McNamara, 1997; Bhullar *et al.*, 2012). However, due to the poor cranial knowledge and fluctuating phylogenetic relationships of basal ceratosaurs from the Early and Middle Jurassic (e.g. Pol and Rauhut, 2012; Tortosa et al., 2013), the early skull shape evolution of Ceratosauria is not currently reproducible. In contrast, the skull of the hypothetical ancestor of Avetheropoda is probably paedomorphic with respect to that of Orionides as shown in the regression analyses (Fig. 4b, c). This trend might extend to the hypothetical ancestor of Coelurosauria, Maniraptoriformes and Maniraptora, leading to a shorter, more tapering snout in lateral view,

687 smaller antorbital fenestrae, enlarged subcircular orbits, and a more gracile postrostral region,
688 resembling the skull shape of the juvenile megalosaurid *Sciurumimus*. These findings may
689 indicate that the paedomorphic trend hypothesized for Eumaniraptora by Bhullar *et al.* (2012)
690 reaches back into the early evolution of Avetheropoda, and that basal coelurosaurs in fact
691 represent "miniaturized" tetanurans, conserving juvenile characters in adult individuals. A
692 similar trend is found for body size evolution in theropods, showing a successive decrease in
693 body size within Avetheropoda (Novas et al., 2012; Dececchi & Larsson, 2013; Lee et al. 2014).
694 In contrast to this supposed early paedomorphic trend, the ancestral shape reconstruction reveals
695 that the skulls of allosauroids become secondarily more robust in relation to the hypothetical
696 ancestor of Avetheropoda, supporting cranial peramorphosis (see Canale *et al*., 2014). This
697 might also be the case for large-bodied tyrannosaurids (see Long & McNamara, 1997; Bhullar *et*
698 *al.*, 2012), although the current regression analyses could not find such a signal for both groups
699 (see below). Bhullar *et al.* (2012) suggested a multi-step progenetic paedomorphosis for skull
700 shape of Paraves and basal birds, with modular peramorphic trends related to beak formation,
701 and further peramorphic trends for secondarily large-bodied troodontids and dromaeosaurids.
702 These heterochronic changes were supported by trends regarding body size evolution (Turner *et*
703 *al.*, 2007; Dececchi & Larrson 2013; Lee et al. 2014) and growth patterns (Erickson *et al*., 2009)
704 found within Eumaniraptora. However, as it is the case for Sauropodomorpha, various trends
705 seen in skull shape evolution of theropods need to be verified in the future regarding possible
706 heterochrony on the basis of new material of both juvenile and adult specimens.
707
708 **Functional and ecological implications**

709 The major differences in cranial shape found here clearly affect dietary preferences and
710 functional constraints. The robust morphology of the postorbital region and the oval orbit in
711 peramorphic skulls was previously discussed in relation to the generation of higher bite forces
712 (Henderson, 2002; Foth & Rauhut, 2013a). However, these functional constraints go hand in
713 hand with a decrease in cranial disparity (Brusatte *et al.*, 2012). Paedomorphic changes in the
714 orbital and postorbital regions were discussed in relation to visual elaboration and brain
715 enlargement (Bhullar *et al*., 2012), and may have played an important role in nocturnal activity
716 (Schmitz & Motani, 2011) or the evolution of flight within Paraves (Balanoff *et al*., 2013). On
717 the other hand, large and circular orbits might simply correlate with reduced mechanical stresses
718 during biting (Henderson, 2002), which have been suggested to also influence size and shape of
719 the external naris, antorbital fenestra and infratemporal fenestra (Witmer, 1997; Witzel &
720 Preuschoft, 2005; Witzel *et al*., 2011).
721
722 Both ontogenetic and phylogenetic variations in snout shape are likely related to dietary
723 preferences (Brusatte *et al.* 2012; Foth & Rauhut 2013; see above), in which the shape of
724 premaxillae and maxillae partly determines the number and size of teeth (Henderson &
725 Weishampel, 2002). Various examples of ontogenetic changes in the morphology and number of
726 teeth are documented in Saurischia, including the basal sauropodomorph *Massospondylus*,
727 coelophysoids (Colbert, 1989), basal tetanurans (Rauhut & Fechner, 2005; Rauhut *et al.*, 2012),
728 tyrannosaurids (Carr, 1999; Tsuihiji *et al.*, 2011) and maniraptorans (Kundrát *et al*., 2008; Bever
729 & Norell, 2009). Based on these observations the evolutionary increase in the number of teeth
730 has been interpreted as peramorphic (Bever & Norell, 2009). Tooth morphology, however, was
731 found to be a stronger indicator of diet than the shape of the snout itself (see Smith, 1993;

732 Barrett, 2000; Barrett, Butler & Nesbitt, 2011; Zanno & Makovicky, 2011; Foth & Rauhut,
733 2013a; Hendrickx & Mateus, 2014). In this context, Rauhut *et al.* (2012) hypothesised based on
734 the similarities in the dentition of the juvenile megalosaurid *Sciurumimus*, adult compsognathids
735 (Stromer, 1934; Currie & Chen, 2001; Peyer, 2006) and adult dromaeosaurids (Xu & Wu, 2001;
736 Norell *et al.*, 2006), that strongly recurved crowns with reduced or no mesial serrations may be
737 paedomorphic in the latter two taxa. This heterochrony probably results from the decrease of
738 body size observed in coelurosaurs (see above) and indicates an evolutionary shift in dietary
739 preferences to smaller prey (see also Zanno & Makovicky, 2011).
740
741 **Limitations**
742 As is common in vertebrate paleontology, the current study has a limited sample size when
743 compared with extant neontological data sets (Brown & Vavrek, 2015). The current results are
744 necessarily preliminary and must be viewed with caution especially because the sampling of
745 ontogenetic trajectories is considerably lower than the sampling of adult individuals.
746 Furthermore, trajectories are constructed using a single juvenile and adult specimen, with no
747 intermediate forms. A single multistage example for *Tyrannosaurus* presented by Bhullar *et al.*
748 (2012) has shown that during ontogeny the trajectory can change its direction considerably in a
749 multivariate PCA plot. This, in turn, has an important impact on the length of the trajectory and
750 its angle in relation to other trajectories. However, in regression analyses the difference with a
751 two-stage approach should be less substantial as multivariate shape information is transformed
752 into a single variable of shape for each stage with respect to its centroid size. The poor sample of
753 juveniles is a result of rarity and poor preservation in the fossil record, which seems to be due to
754 a number of factors, including preferred hunting of juveniles by predators (Hone & Rauhut,

755 2010) and a smaller likelihood of preservation, discovery, and collection because juveniles have
756 smaller body sizes and more fragile bones than adults (Brown *et al.*, 2013). Thus, due to small
757 sample sizes, the statistical power of our analyses is generally low (see Cumming, Fidler &
758 Vaux, 2007), limiting the explanatory power of our results. On the other hand, Brown & Vavrek
759 (2015) recently demonstrated that the number of positive and negative allometries is
760 underestimated in smaller samples in both paleontological and neontological data sets.
761
762 Another issue affecting our results is that the juvenile individuals sampled here are all of
763 different early ontogenetic stages. The juvenile *Massospondylus* represents a composite of
764 several embryos close to hatching (Reisz *et al*., 2010); the megalosaurid taxon (i.e. *Sciurumimus*
765 *albersdoerferi*) is an early juvenile and its exact age could not be determined (Rauhut *et al*.,
766 2012); the age of the *Coelophysis* juvenile reconstructed is approximately one year old
767 (estimated by Colbert, 1990; Rinehart *et al*., 2009); the juvenile *Tarbosaurus* specimen is two to
768 three years old (Tsuihiji *et al*., 2011); and the juvenile *Allosaurus* is likely five to seven years old
769 (estimated based on Bybee, Lee & Lamm, 2006; Loewen, 2009). Thus, the different ontogenetic
770 stages of the juvenile specimens and the small number of individuals for each ontogenetic series
771 most likely affected the length, but maybe also the slope of the calculated trajectories (and thus
772 the angles between the trajectories) (see Cardini & Elton, 2007), including that of the
773 hypothetical ancestors. Furthermore, the uncertainty regarding the age of the specimens leads to
774 another weak point, as specimen age was not used to characterize the ontogenetic trajectories
775 (see above), which is a common problem in paleontology (e.g. McKinney, 1986; Klingenberg,
776 1998, Gould, 2000, Schoch, 2010; Bhullar *et al.*, 2012). In consequence, the applied regression
777 analyses explored allometry and not heterochrony (see Klingenberg & Spence, 1993;

778 Klingenberg, 1998). The substitution of age by size, however, would imply similar growth
779 dynamics (i.e. proportionality between age and size) between ancestors and descendants, which
780 would consequently ignore heterochronic processes related to growth rates (i.e. progenesis and
781 acceleration). Although dinosaurs generally have higher growth rates compared to other non-
782 avian reptiles, histological studies reveal that growth rates are not identical (Erickson, Rogers &
783 Yerby, 2001, 2004; Padian, de Ricqlès & Horner, 2001; Sander et al., 2004; Erickson *et al.*,
784 2009; Grady et al., 2014; Werner & Griebeler, 2014). Therefore, allometric patterns cannot be
785 used to infer heterochrony beyond paedomorphosis and peramorphosis as argued by Klingenberg
786 & Spence (1993) and Klingenberg (1998). Taking the uncertainties related to the lengths and
787 slopes of the ontogenetic trajectories (due to incomplete ontogenetic series) and statistical
788 uncertainties (due to the small sample size) into account, the classifications of underlying
789 heterochronic processes would be misleading and probably erroneous.
790
791 In the current study, the interpretations of paedomorphosis and peramorphosis rely on the
792 significant shape differences between adult individuals of the ontogenetic trajectories expressed
793 by shape vectors in the regression analyses, for which the multivariate shape data were
794 transformed into a univariate shape variable. These differences are affected by type of shape
795 variable, but more importantly by the ancestral shapes, which in turn depend on the phylogenetic
796 relationships, the algorithm of time calibration (e.g. Bapst, 2014) and the method of
797 reconstruction (e.g. Martins, 1999; Webster & Purvis, 2001). Thus, one has to be aware that the
798 application of different methods could result in slightly different ancestral shapes, affecting the
799 value of the shape variable. However, because the current sample covers all major linages of
800 basal saurischians except of crested taxa, which were found to impact the ancestral shape of the
801 skull roofs significantly (see Fig. S5, Table S6 in the Supplementary Information), the results of

802 the ancestral reconstruction of adult individuals are viewed as valid. By using two different
803 shape variables (Regression score and Euclidean distance), it was possible to confirm significant
804 results through multiple methods.
805
806 The undefined trend found for *Tarbosaurus* in relation to the hypothetical ancestor of
807 Avetheropoda illustrates the limitations of our analyses. Our result is seemingly contradictory to
808 previous hypotheses and our ancestral shape reconstruction, which proposed peramorphosis as
809 the main driver of skull evolution in large-bodied tyrannosaurids (see above, Long &
810 McNamara, 1997, Bhullar *et al.*, 2012). As stated above, this result is most likely related to the
811 small sample size of ontogenetic trajectories as skulls with elongated and slender snouts are
812 considered to be peramorphic on the basis of the regression analyses. The inclusion of more
813 ontogenetic trajectories of large-bodied theropods would probably change this result in favour of
814 a trend towards a deeper snout. Furthermore, large-bodied tyrannosaurids like *Tarbosaurus*
815 descended from small-bodied coelurosaurian ancestors (Xu *et al*., 2004, 2006; Brusatte *et al*.,
816 2010; Rauhut *et al*., 2010; Benson *et al*., 2014), which means that the hypothetical inclusion of
817 an ontogenetic trajectory of a small-bodied basal coelurosaur (e.g. *Compsognathus*, *Dilong*,
818 *Haplocheirus*) and a respective hypothetical ancestor of Coelurosauria would probably change
819 the current results, leading to a secondary peramorphic trend in Late Cretaceous tyrannosaurids,
820 as suggested by previous authors. Thus, this result is very likely an artefact of incomplete
821 sampling. In this context, the limited number of ontogenetic series of basal sauropodomorphs
822 results only in a rough trend regarding the relationship between cranial ontogeny and evolution,
823 which cannot be extended to more general patterns in the skull shape evolution of basal
824 sauropods.

825

826 **Conclusions**

827 The importance of heterochrony in non-avian dinosaur skull evolution is a relatively new
828 concept (see Long & McNamara, 1997; Bhullar *et al*., 2012). This study quantitatively assesses
829 the impact of skull heterochrony across early saurischian evolution, allowing testing some of the
830 heterochronic trends proposed by Bhullar *et al.* (2012) and further highlights different vantages
831 of using morphometric data to elucidate heterochronic trends. We estimated hypothetical
832 ontogenetic trajectories in Saurischia, Neotheropoda, Orionides, and Avetheropoda using
833 ontogenetic trajectories of *Massospondylus*, *Coelophysis*, a megalosaurid taxon, *Allosaurus* and
834 *Tarbosaurus*. When compared using PCA, the ontogenetic trajectories of the terminal taxa show
835 great variation in length and direction, but still follow some very general patterns, including a
836 relatively elongated and dorsoventrally deeper preorbital region, decrease in orbit size and
837 increase in jugal robustness. General peramorphic skulls include more elongate and slender
838 snouts, elongate antorbital fenestrae, oval orbits, dorsoventrally shallower post-rostral regions,
839 and more massive maxillae, jugals, and postorbitals. Paedomorphic skulls show the opposite
840 features. The shape changes from the hypothetical ancestor of Saurischia to *Massospondylus*
841 were paedomorphic, as previously suggested by Bhullar *et al.* (2012). In contrast, skull evolution
842 of basal theropod taxa was probably affected by peramorphic trends. However, Avetheropoda
843 showed paedomorphic changes compared to Orionides. This might indicate that the
844 paedomorphic trend found for Eumaniraptora (see Bhullar *et al*., 2012) may reach back into the
845 early evolution of Avetheropoda. The hypothesized peramorphic evolution for skull shape of
846 allosaurids and tyrannosaurids could not be supported by the current study, but this probably
847 resulted from the small sample size of ontogenetic trajectories. Although our data showed

minimal differences between our crested-taxa and non-crested taxa data sets and semi-landmark and no semi-landmark data sets, it is important to fully evaluate all possible sources of trends, especially when working with a small data set. As stated above, our study is hampered by the preservation of the fossil record (mainly the poor sample of complete juvenile specimens) and more finds will help to elucidate other evolutionary patterns related to heterochrony. With a larger number of taxa comprising juvenile and adult stages it will be possible to further test heterochronic hypotheses within Saurischia in more detail, and eliminate artefacts related to sample size. Future studies may also examine ontogenetic histories of individual taxa that have reasonably complete ontogenetic samples, such as *Coelophysis*, to evaluate which factors (dietary preference, heterochrony, etc.) drive shape change in individual taxa. A larger number of studies using geometric morphometrics for individual taxa as well as a more complete sampling within Saurischia are necessary to more completely assess the importance of heterochronic processes in both sauropodomorph and theropod skull shape. In addition, it would be of value to explore modularity in saurischian skulls to project the investigation of heterochronic processes to particular skull regions. In sum, this study demonstrates that heterochrony played an important role in basal non-avian saurischian skull evolution building upon previous studies (Bhullar et al., 2012).

Acknowledgements:

We thank Oliver Rauhut (Bayerische Staatssammlung für Paläontologie und Geologie, München), Miriam Zelditch (University of Michigan), Johannes Knebel (Ludwig Maximilians University, München), Stefan Richter (University of Rostock), Walter Joyce and Eduardo Ascarrunz (both University of Fribourg) for discussion, and Michel Laurin (Sorbonne

871 Universités, Paris) for comments on an earlier version of the manuscript. We further thank
872 Matthew Lamanna (Carnegie Museum of Natural History, Pittsburgh), Alex Downs (Ruth Hall
873 Museum, Ghost Ranch), David Gillette (Museum of Northern Arizona, Flagstaff) and Xu Xing
874 (Institute of Vertebrate Paleontology and Paleoanthropology, Beijing) for access to collections.
875 This study benefitted especially from critical comments of Jesús Marugán-Lobón (Universidad
876 Autónoma de Madrid) and three anonymous reviewers.
877

878 **References**

879 Adams DC. 2014. A generalized K statistic for estimating phylogenetic signal from shape and
880 other high-dimensional multivariate data. *Systematic Biology* 63:685–697.
881 Adams DC, Otárola-Castillo E. 2013. geomorph: an R package for the collection and analysis of
882 geometricmorphometric shape data. *Methods in Ecology and Evolution* 4:393–399.
883 Adams DC, Rohlf FJ, Slice DE. 2004. Geometric morphometrics: ten years of progress
884 following the "revolution." *Italian Journal of Zoology* 71:5–16.
885 Adams DC, Rohlf FJ, Slice DE. 2013. A field comes of age: geometric morphometrics in the
886 21st century. *Hystrix, the Italian Journal of Mammalogy* 24:7–14.
887 Alberch P, Gould SJ, Oster GF, Wake DB. 1979. Size and shape in ontogeny and phylogeny.
888 *Paleobiology* 5:296–317.
889 Balanoff AM, Rowe TB. 2007. Osteological description of an embryonic skeleton of the extinct
890 elephant bird, *Aepyornis* (Palaeognathae: Ratitae). *Journal of Vertebrate Paleontology*
891 27:1–53.
892 Balanoff AM, Bever GS, Rowe TB, Norell MA. 2013. Evolutionary origins of the avian brain.
893 *Nature* 201:93–96.

894 Bapst DW. 2014. Assessing the effect of time-scaling methods on phylogeny-based analyses in
895 the fossil record. *Paleobiology* 40:331–351.
896 Barrett PM. 2000. Prosauropod dinosaurs and iguanas: speculations on the diets of extinct
897 reptiles. In: Sues H-D ed. *Evolution of herbivory in terrestrial vertebrates*. Cambridge:
898 Cambridge University Press, 42–78.
899 Barrett PM, Rayfield EJ. 2006. Ecological and evolutionary implications of dinosaur feeding
900 behaviour. *Trends in Ecology and Evolution* 21:217–224.
901 Barrett PM, Butler RJ, Nesbitt SJ. 2011. The roles of herbivory and omnivory in early dinosaur
902 evolution. *Earth and Environmental Science Transactions of the Royal Society of*
903 *Edinburgh* 101:383–396.
904 Benson RBJ, Campione NE, Carrano MT, Mannion PD, Sullivan C, Upchurch P, Evans SE.
905 2014. Rates of dinosaur body mass evolution indicate 170 million years of sustained
906 ecological innovation on the avian stem lineage. *PloS Biology* 12:e1001853.
907 Berge C, Penin X. 2004. Ontogenetic allometry, heterochrony, and interspecific differences in
908 the skull of african apes, using tridimensional procrustes analysis. *American Journal of*
909 *Physical Anthropology* 124:124–138.
910 Bever GS, Norell MA. 2009. The perinate skull of *Byronosaurus* (Troodontidae) with
911 observations on the cranial Ontogeny of paravian theropods. *American Museum Novitates*
912 3657:1–51.
913 Bhullar B-A, Marugán-Lobón J, Racimo F, Bever GS, Rowe TB, Norell MA, Abzhanov A.
914 2012. Birds have paedomorphic dinosaur skulls. *Nature* 487:223–226.

915 Bhullar B-A. 2012. A phylogenetic approach to ontogeny and heterochrony in the fossil record:
916 cranial evolution and development in anguimorphan lizards (Reptilia: Squamata). *Journal*
917 *of Experimental Zoology (MOL DEV EVOL)* 318B:521–530.
918 Blomberg S, Garland TJ, AR I. 2003. Testing for phylogenetic signal in comparative data:
919 behavioral traits are more labile. *Evolution* 57:717–745.
920 Bonnan MF. 2004. Morphometric analysis of humerus and femur shape in Morrison sauropods:
921 implications for functional morphology and paleobiology. *Paleobiology* 30:444–470.
922 Bookstein FL. 1991. *Morphometric tools for landmark data*. Cambridge: Cambridge University
923 Press.
924 Bookstein FL, Schäfer K, Prossinger H, Seidler H, Fiedler M, Stringer C, Weber GW, Arsuaga J-
925 L, Slice DE, Rohlf FJ, Recheis W, Mariam AJ, Marcus LF. 1999. Comparing frontal
926 cranial profiles in archaic and modern *Homo* by morphometric analysis. *The Anatomical*
927 *Record* 257:217–224.
928 Brown CM, Evans DC, Campione NE, O’ Brien LJ, Eberth DA. 2013. Evidence for taphonomic
929 size bias in the Dinosaur Park Formation (Campanian, Alberta), a model Mesozoic
930 terrestrial alluvial‐paralic system. *Palaeogeography, Palaeoclimatology, Palaeoecology*
931 372:108–122.
932 Brown CM, Vavrek MJ. 2015. Small sample sizes in the study of ontogenetic allometry;
933 implications for palaeobiology. *PeerJ* 3:e818.
934 Brusatte SL, Benton MJ, Ruta M, Lloyd GT. 2008. Superiority, competition, and opportunism in
935 the evolutionary radiation of dinosaurs. *Science* 321:1485–1488.

936 Brusatte SL, Norell MA, Carr TD, Erickson GM, Hutchinson JR, Balanoff AM, Bever GS,
937 Choiniere JN, Makovicky PJ, Xu X. 2010. Tyrannosaur paleobiology: new research on
938 ancient exemplar organisms. *Science* 329:1481–1485.
939 Brusatte SL. 2011. Calculating the tempo of morphological evolution: rates of discrete character
940 change in a phylogenetic context. In: Elewa AMT ed. *Computational Paleontology*.
941 Heidelberg: Springer, 53–74.
942 Brusatte SL, Carr TD, Norell MA. 2012. The osteology of *Alioramus*, a gracile and long-snouted
943 tyrannosaurid (Dinosauria: Theropoda) from the Late Cretaceous of Mongolia. *Bulletin of*
944 *the American Museum of Natural History* 366:1–197.
945 Brusatte SL, Montanari S, Sakamoto M, Harcourt-Smith WEH. 2012. The evolution of cranial
946 form and function in theropod dinosaurs: insight from geometric morphometrics. *Journal*
947 *of Evolutionary Biology* 25:365–377.
948 Butler RJ, Goswami A. 2008. Body size evolution in Mesozoic birds: little evidence for Cope's
949 rule. *Journal of Evolutionary Biology* 21:1673–1682.
950 Bybee PJ, Lee AH, Lamm E-T. 2006. Sizing the Jurassic theropod dinosaur *Allosaurus*:
951 assessing growth strategy and evolution of ontogenetic scaling of limbs. *Journal of*
952 *Morphology* 267:347–359.
953 Cabreira SF, Schultz CL, Bittencourt JS, Soares MB, Fortier DC, Silva LR, Langer MC. 2011.
954 New stem-sauropodomorph (Dinosauria, Saurischia) from the Triassic of Brazil.
955 *Naturwissenschaften* 98:1035–1040.
956 Campione NE, Evans DC. 2011. Cranial growth and variation in edmontosaurs (Dinosauria:
957 Hadrosauridae): implications for Latest Cretaceous megaherbivore diversity in North
958 America. *PLoS ONE* 6:e25186.

959 Canale IC, Novas FE, Salgado L, Coria RA. 2014. Cranial ontogenetic variation in *Mapusaurus*
960 *roseae* (Dinosauria: Theropoda) and the probable role of heterochrony in
961 carcharodontosaurid evolution. *Paläontolologische Zeitschrift*:1–11.
962 Cardini A, Elton S. 2007. Sample size and sampling error in geometric morphometric studies of
963 size and shape. *Zoomorphology* 126:121–134.
964 Carr TD. 1999. Craniofacial ontogeny in Tyrannosauridae (Dinosauria, Coelurosauria). *Journal*
965 *of Vertebrate Paleontology* 19:497–520.
966 Carr TD, Williamson TE. 2004. Diversity of late Maastrichtian Tyrannosauridae (Dinosauria:
967 Theropoda) from western North America. *Zoological Journal of the Linnean Society*
968 142:479–523.
969 Carrano MT, Benson RBJ, Sampson SD. 2012. The phylogeny of Tetanurae (Dinosauria:
970 Theropoda). *Journal of Systematic Palaeontology* 10:211–300.
971 Chinnery B. 2004. Morphometric analysis of evolutionary trends in the ceratopsian postcranial
972 skeleton. *Journal of Vertebrate Paleontology* 24:591–609.
973 Chinsamy A. 1993. Bone histology and growth trajectory of the prosauropod dinosaur
974 *Massospondylus carinatus* Owen. *Modern Geology* 18:319–329.
975 Colbert EH. 1989. The Triassic dinosaur *Coelophysis*. *Museum of Northern Arizona Bulletin* 57:
976 1–160.
977 Colbert EH. 1990. Variation in *Coelophysis bauri*. In: Carpenter K, Currie PJ eds. *Dinosaur*
978 *systematics: approaches and perspectives*. Cambridge: Cambridge University Press, 81–
979 90.
980 Collyer ML, Adams DC. 2007. Analysis of two-state multivariate phenotypic change in
981 ecological studies. *Ecology* 88:683–692.

982 Corti M. 1993. Geometric Morphometrics: an extension of the revolution. *Trends in Ecology and*
983 *Evolution* 8:302–303.
984 Cumming G, Fidler F, Vaux DL. 2007. Error bars in experimental biology. *The Journal of Cell*
985 *Biology* 177:7–11.
986 Currie PJ, Chen P. 2001. Anatomy of *Sinosauropteryx prima* from Liaoning, northeastern China.
987 *Canadian Journal of Earth Sciences* 38:1705–1727.
988 Dal Sasso C, Maganuco S. 2011. *Scipionyx samniticus* (Theropoda: Compsognathidae) from the
989 Lower Cretaceous of Italy. *Memorie della Società Italiana di Scienze Naturali e del Museo*
990 *Civico di Storia Naturale di Milano* 37:1–281.
991 Dececchi TA, Larsson HCE. 2013. Body and limb size dissociation at the origin of birds:
992 uncoupling allometric constraints across a macroevolutionary transition. *Evolution*
993 67:2741–2752.
994 Drake AG. 2011. Dispelling dog dogma: an investigation of heterochrony in dogs using 3D
995 geometric morphometric analysis of skull shape. *Evolution & Development* 13:204–213.
996 Drake AG, Klingenberg CP. 2008. The pace of morphological change: historical transformation
997 of skull shape in St Bernard dogs. *Proceedings of the Royal Society B* 275:71–76.
998 Erickson GM, Rogers KC, Yerby SA. 2001. Dinosaur growth patterns and rapid avian growth
999 rates. *Nature* 412:429–432.
1000 Erickson GM, Makovicky PJ, Currie PJ, Norell MA, Yerby SA, Brochu CA. 2004. Gigantism
1001 and comparative life-history parameters of tyrannosaurid dinosaurs. *Nature* 430:772–775.
1002 Erickson GM, Rauhut OWM, Zhou Z, Turner AH, Inouye BD, Hu D, Norell MA. 2009. Was
1003 dinosaurian physiology inherited by birds? Reconciling slow growth in *Archaeopteryx*.
1004 *PLoS ONE* 4:e7390.

1005 Evans DC. 2010. Cranial anatomy and systematics of *Hypacrosaurus altispinus*, and a
1006 comparative analysis of skull growth in lambeosaurine hadrosaurids (Dinosauria:
1007 Ornithischia). *Zoological Journal of the Linnean Society* 159:398–434.
1008 Ezcurra MD. 2007. The cranial anatomy of the coelophysoid theropod *Zupaysaurus rougieri*
1009 (Upper Triassic, Argentina). *Historical Biology* 19:185−202.
1010 Ezcurra MD. 2012. Phylogenetic analysis of Late Triassic-Early Jurassic neotheropod dinosaurs:
1011 implications for the early theropod radiation. *Journal of Vertebrate Paleontology, Program*
1012 *and Abstracts* 32:91.
1013 Ezcurra MD, Butler RJ. 2015. Post-hatchling cranial ontogeny in the Early Triassic diapsid
1014 reptile *Proterosuchus fergusi*. *Journal of Anatomy*:1–16.
1015 Ezcurra MD, Novas FE. 2007. Phylogenetic relationships of the Triassic theropod *Zupaysaurus*
1016 *rougieri* from NWArgentina. *Historical Biology* 19:35–72.
1017 Fink WL. 1982. The conceptual relationship between ontogeny and phylogeny. *Paleobiology*
1018 8:254–264.
1019 Forasiepi AM, Sánchez-Villagra MR. 2014. Heterochrony, dental ontogenetic diversity, and the
1020 circumvention of constraints in marsupial mammals and extinct relatives. *Paleobiology*
1021 40:222–237.
1022 Foth C. 2013. Ontogenetic, macroevolutionary and morphofunctional patterns in archosaur
1023 skulls: a morphometric approach. *Ludwig-Maximilians-Universität, München*.
1024 Foth C, Rauhut OWM. 2013a. Macroevolutionary and morphofunctional patterns in theropod
1025 skulls: a morphometric approach. *Acta Palaeontologica Polonica* 58:1–16.

1026 Foth C, Rauhut OWM. 2013b. The good, the bad, and the ugly: the influence of skull
1027 reconstructions and intraspecific variability in studies of cranial morphometrics in
1028 theropods and basal saurischians. *PLoS ONE* 8:e72007.
1029 Frederickson JA, Tumarkin-Deratzian AR. 2014. Craniofacial ontogeny in *Centrosaurus*
1030 *apertus*. *PeerJ* 2:e252.
1031 Fritsch M, Bininda-Emonds ORP, Richter S. 2013. Unraveling the origin of Cladocera by
1032 identifying heterochrony in the developmental sequences of Branchiopoda. *Frontiers in*
1033 *Zoology* 10:35.
1034 Gerber S, Neige P, Eble GJ. 2007. Combining ontogenetic and evolutionary scales of
1035 morphological disparity: a study of early Jurassic ammonites. *Evolution & Development*
1036 9:472–482.
1037 Gould SJ. 1977. *Ontogeny and phylogeny*. Cambridge: Harvard University Press.
1038 Gould SJ. 2000. Of coiled oysters and big brains: how to rescue the terminology of heterochrony,
1039 now gone astray. *Evolution & Development* 2:241–248.
1040 Gow CE, Kitching JW, Raath MA. 1990. Skulls of the prosauropod dinosaur *Massospondylus*
1041 *carinatus* Owen in the collections of the Bernand Price Institute for Palaeontological
1042 Research. *Palaeontologia Africana* 27:45–58.
1043 Gower JC. 1975. Generalized Procrustes analysis. *Psychometrika* 40:33–51.
1044 Grady JM, Enquist BJ, Dettweiler-Robinson E, Wright NA, Smith FA. 2014. Evidence for
1045 mesothermy in dinosaurs. *Science* 344:1268–1272.
1046 Guenther MF. 2009. Influence of sequence heterochrony on hadrosaurid dinosaur postcranial
1047 development. *The Anatomical Record* 292:1427–1441.

1048 Hammer O, Harper DAT, Ryan PD. 2001. PAST: paleontological statistics software package for
1049 education and data analysis. *Palaeontologia Electronica* 4:1–9.
1050 Hedrick BP, Dodson P. 2013. Lujiatun psittacosaurids: understanding individual and taphonomic
1051 variation using 3D geometric morphometrics. *PLoS ONE* 8:e69265.
1052 Henderson DM. 2002. The eyes have it: the sizes, shapes, and orientations of theropod orbits as
1053 indicators of skull strength and bite force. *Journal of Vertebrate Paleontology* 22:766–778.
1054 Henderson DM, Weishampel DB. 2002. Convergent evolution of the maxilla-dental-complex
1055 among carnivorous archosaurs. *Senckenbergiana lethaea* 82:77–92.
1056 Hendrickx C, Mateus O. 2014. Abelisauridae (Dinosauria: Theropoda) from the Late Jurassic of
1057 Portugal and dentition-based phylogeny as a contribution for the identification of isolated
1058 theropod teeth. *Zootaxa* 3759:1–74.
1059 Hennig W. 1966. *Phylogenetic systematics*. Urbana: University of Illinois Press.
1060 Hone DWE, Naish D, Cuthill I. 2012. Does mutual sexual selection explain the evolution of head
1061 crests in pterosaurs and dinosaurs? *Lethaia* 45:139–156.
1062 Hone DWE, Rauhut OWM. 2010. Feeding behaviour and bone utilization by theropod dinosaurs.
1063 *Lethaia* 43:232–244.
1064 Horner JR, Goodwin MB. 2006. Major cranial changes during *Triceratops* ontogeny.
1065 *Proceedings of the Royal Society B* 273:2757–2761.
1066 Horner JR, Goodwin MB. 2009. Extreme cranial ontogeny in the Upper Cretaceous dinosaur
1067 *Pachycephalosaurus*. *PLoS ONE* 4:e7626.
1068 Hübner TR, Rauhut OWM. 2010. A juvenile skull of *Dysalotosaurus lettowvorbecki*
1069 (Ornithischia: Iguanodontia), and implications for cranial ontogeny, phylogeny, and

taxonomy in ornithopod dinosaurs. *Zoological Journal of the Linnean Society* 160:366–396.

Irmis RB. 2011. Evaluating hypotheses for the early diversification of dinosaurs. *Earth and Environmental Science Transactions of the Royal Society of Edinburgh* 101:397–426.

Jackson DA. 1993. Stopping rules in principal components analysis: a comparison of heuristical and statistical approaches. *Ecology* 74:2204–2214.

Klein N, Sander PM. 2007. Bone histology and growth of the prosauropod dinosaur *Plateosaurus engelhardti* von Mayer, 1837 from the Norian bonebeds of Trossingen (Germany) and Frick (Switzerland). *Special Papers in Palaeontology* 77:169–206.

Klingenberg CP. 1998. Heterochrony and allometry: the analysis of evolutionary change in ontogeny. *Biological Reviews* 73:79–123.

Klingenberg CP. 2011. MorphoJ: an integrated software package for geometric morphometrics. *Molecular Ecology Resources* 11:353–357.

Klingenberg CP, Gidaszewski NA. 2010. Testing and quantifying phylogenetic signals and homoplasy in morphometric data. *Systematic Biology* 59:245–261.

Klingenberg CP, Spence JR. 1993. Heterochrony and allometry: lessons from the water strider genus *Limnoporus*. *Evolution* 47:1834–1853.

Kundrát M, Cruickshank ARI, Manning TW, Nudds J. 2008. Embryos of therizinosauroid theropods from the Upper Cretaceous of China: diagnosis and analysis of ossification patterns. *Acta Zoologica (Stockholm)* 89:231–251.

Langer MC, Ezcurra MD, Bittencourt JS, Novas FE. 2010. The origin and early evolution of dinosaurs. *Biological Reviews* 85:55–110.

1092 Laurin M. 2004. The evolution of body size, Cope's rule and the origin of amniotes. *Systematic*
1093 *Biology* 53:594–622.
1094 Lautenschlager S. 2014. Morphological and functional diversity in therizinosaur claws and the
1095 implications for theropod claw evolution. *Proceedings of the Royal Society B*
1096 281:20140497.
1097 Lee MSY, Cau A, Naish D, Dyke GJ. 2014. Sustained miniaturization and anatomical innovation
1098 in the dinosaurian ancestors of birds. *Science* 345:562–566.
1099 Li D, Norell MA, Gao K, Smith ND, Makovicky PJ. 2010. A longirostrine tyrannosauroid from
1100 the Early Cretaceous of China. *Proceedings of the Royal Society B* 277:183–190.
1101 Lieberman DE, Carlo J, Ponc de Leóon M, Zollikofer CPE. 2007. A geometric morphometric
1102 analysis of heterochrony in the cranium of chimpanzees and bonobos. *Journal of Human*
1103 *Evolution* 52:647–662.
1104 Loewen MA. 2009. *Variation in the Late Jurassic theropod dinosaur* Allosaurus*: ontogenetic,*
1105 *functional, and taxonomic implications*. University of Utah, Salt Lake City.
1106 Loewen MA, Irmis RB, Sertich JJW, Currie PJ, Sampson SD. 2013. Tyrant dinosaur evolution
1107 tracks the rise and fall of Late Cretaceous oceans. *PLoS ONE* 8:e79420.
1108 Long JA, McNamara KJ. 1997. Heterochrony: the key to dinosaur evolution. In: Wolberg DL,
1109 Stumps E, Rosenberg GD eds. *Dinofest International*. Philadelphia: Academy of Natural
1110 Sciences, 113–123.
1111 Lü J, Yi L, Brusatte SL, Yang L, Li H, Chen L. 2014. A new clade of Asian Late Cretaceous
1112 long-snouted tyrannosaurids. *Nature Communications* 5:3788.
1113 Maddison WP. 1991. Squared-change parsimony reconstructions of ancestral states for
1114 continuous-valued characters on a phylogenetic tree. *Systematic Zoology* 40:304–314.

1115 Maddison WP, Maddison DR. 2009. Mesquite: A modular system of evolutionary analysis.
1116 Version 2.72.
1117 Madsen JHJ, Welles SP. 2000. *Ceratosaurus* (Dinosauria, Theropoda), a revised osteology. *Utah*
1118 *Geology Survey Miscellaneous Publication* 00-2:1–80.
1119 Maiorini L, Farke AA, Kotsakis T, Piras P. 2015. Males resemble females: re-evaluating sexual
1120 dimorphism in *Protoceratops andrewsi* (Neoceratopsia, Protoceratopsidae). *PLoS ONE*
1121 10:e0126464.
1122 Mallon JC, Holmes R, Eberth DA, Ryan MJ, Anderson JS. 2011. Variation in the skull of
1123 *Anchiceratops* (Dinosauria, Ceratopsidae) from the Horseshoe Canyon Formation (Upper
1124 Cretaceous) of Alberta. *Journal of Vertebrate Paleontology* 31:1047–1071.
1125 Mallon JC, Ryan MJ, Campbell JA. 2015. Skull ontogeny in *Arrhinoceratops brachyops*
1126 (Ornithischia: Ceratopsidae) and other horned dinosaurs. *Zoological Journal of the*
1127 *Linnean* Society:1–20.
1128 Martínez RN. 2009. *Adeopapposaurus mognai*, gen. et sp. nov. (Dinosauria: Sauropodomorpha),
1129 with comments on adaptations of basal Sauropodomorpha. *Journal of Vertebrate*
1130 *Paleontology* 29:142–164.
1131 Martínez RN, Sereno PC, Alcober OA, Colombi CE, Renne PR, Montañez IP, Currie BS. 2011.
1132 A basal dinosaur from the dawn of the dinosaur era in southwestern Pangaea. *Science*
1133 331:206–210.
1134 Martínez RN, Apaldetti C, Abelin D. 2013. Basal sauropodomorphs from the Ischigualasto
1135 Formation. *Society of Vertebrate Paleontology Memoir* 12:51–69.
1136 Martins EP. 1999. Estimation of ancestral states of continuous characters: a computer simulation
1137 study. *Systematic Biology* 48:642–650.

1138 McKinney ML. 1986. Ecological causation of heterochrony: a test and implications for
1139 evolutionary theory. *Paleobiology* 12:282–289.
1140 McNamara KJ. 1982. Heterochrony and phylogenetic trends. *Paleobiology* 8:130–142.
1141 McNamara KJ, McKinney ML. 2005. Heterochrony, disparity, and macroevolution.
1142 *Paleobiology* 31:17–26.
1143 Mitteroecker P, Gunz P, Weber GW, Bookstein FL. 2004. Regional dissociated heterochrony in
1144 multivariate analysis. *Annals of Anatomy* 186:463–470.
1145 Mitteroecker P, Gunz P. 2009. Advances in geometric morphometrics. *Evolutionary Biology*
1146 36:235–247.
1147 Mitteroecker P, Gunz P, Bookstein FL. 2005. Heterochrony and geometric morphometrics: a
1148 comparison of cranial growth in *Pan paniscus* versus *Pan troglodytes*. *Evolution &*
1149 *Development* 7:244–258.
1150 Molnar RE. 2005. Sexual selection and sexual dimorphism in theropods. In: Carpenter K ed. *The*
1151 *carnivorous dinosaurs*. Bloomington: Indiana University Press, 284–312.
1152 Norell MA, Clark JM, Turner AH, Makovicky PJ, Barsbold R, Rowe TB. 2006. A new
1153 droameosaurid theropod from Ukhaa Tolgod (Ömnögov, Mongolia). *American Museum*
1154 *Novitates* 3545:1–51.
1155 Novas FE, Ezcurra MD, Agnolín FL, Pol D, Ortíz R. 2012. New Patagonian Cretaceous theropod
1156 sheds light about the early radiation of Coelurosauria. *Revista del Museo Argentino de*
1157 *Ciencias Naturales, nueva serie*, 14:57–81.
1158 Padian K, Horner JR. 2011. The evolution of "bizarre structures" in dinosaurs: biomechanics,
1159 sexual selection, social selection or species recognition? *Journal of Zoology* 283:3–17.

1160 Padian K, de Ricqlès AJ, Horner JR. 2001. Dinosaurian growth rates and bird origins. *Nature*
1161 412:405–408.
1162 Paradis E. 2012. *Analysis of phylogenetics and evolution with R*. New York: Springer.
1163 Paradis E, Claude J, Strimmer K. 2004. APE: analyses of phylogenetics and evolution in R
1164 language. *Bioinformatics* 20:289–290.
1165 Peyer K. 2006. A reconsideration of *Compsognathus* from the Upper Tithonian of Canjuers,
1166 southeastern France. *Journal of Vertebrate Paleontology* 26:879–896.
1167 Piras P, Salvi D, Ferrara G, Maiorino L, Delfino M, Pedde L, Kotsakis T. 2011. The role of post-
1168 natal ontogeny in the evolution of phenotypic diversity in *Podarcis* lizards. *Journal of*
1169 *Evolutionary Biology* 24:2705–2720.
1170 Pol D, Rauhut OWM. 2012. A Middle Jurassic abelisaurid from Patagonia and the early
1171 diversification of theropod dinosaurs. *Proceedings of the Royal Society B* 279:3170–3175.
1172 Porfiri JD, Novas FE, Calvo JO, Agnolín FL, Ezcurra MD, Cerda IA. 2014. Juvenile specimen of
1173 *Megaraptor* (Dinosauria, Theropoda) sheds light about tyrannosauroid radiation.
1174 *Cretaceous Research* 51:35–55.
1175 Raff RA. 1996. *The shape of life: genes, development, and the evolution of animal form*.
1176 Chicago: University of Chicago Press.
1177 Rauhut OWM. 2003. The interrelationships and evolution of basal theropod dinosaurs. *Special*
1178 *Papers in Palaeontology* 69:1–213.
1179 Rauhut OWM, Fechner R, Remes K, Reis K. 2011. How to get big in the Mesozoic: the
1180 evolution of the sauropodomorph body plan. In: Klein N, Remes K, Gee CT, Sander PM
1181 eds. *Biology of the sauropod dinosaurs: understanding the life of giants*. Bloomington:
1182 Indiana University Press, 119–149.

1183 Rauhut OWM, Foth C, Tischlinger H, Norell MA. 2012. Exceptionally preserved juvenile
1184 megalosauroid theropod dinosaur with filamentous integument from the Late Jurassic of
1185 Germany. *Proceedings of the National Academy of Sciences* 109:11746–11751.
1186 Rauhut OWM, Fechner R. 2005. Early development of the facial region in a non-avian theropod
1187 dinosaur. *Proceedings of the Royal Society B* 272:1179–1183.
1188 Rauhut OWM, Milner AC, Moore-Fay S. 2010. Cranial osteology and phylogenetic position of
1189 the theropod dinosaur *Proceratosaurus bradleyi* (Woodward, 1910) from the Middle
1190 Jurassic of England. *Zoological Journal of the Linnean Society* 158:155–195.
1191 R-Development-Core-Team. 2011. R: a language and environment for statistical computing.
1192 Reilly SM, Wiley EO, Meinhardt DJ. 1997. An integrative approach to heterochrony: the
1193 distinction between interspecific and intraspecific phenomena. *Biological Journal of the*
1194 *Linnean Society* 60:119–143.
1195 Reisz RR, Evans DC, Sues H-D, Scott D. 2010. Embryonic skeletal anatomy of the
1196 sauropodomorph dinosaur *Massospondylus* from the Lower Jurassic of South Africa.
1197 *Journal of Vertebrate Paleontology* 30:1653–1665.
1198 Rinehart LF, Lucas SG, Heckert AB, Spielmann JA, Celeskey MD. 2009. The paleobiology of
1199 *Coelophysis bauri* (Cope) from the Upper Triassic (Apachean) Whitaker quarry, New
1200 Mexico, with detailed analysis of a single quarry block. *New Mexico Museum of Natural*
1201 *History and Science, Bulletin* 45:1–260.
1202 Rohlf FJ. 2005. tpsDig, digitize landmarks and outlines, version 2.05.
1203 Rohlf FJ, Marcus LF. 1993. A revolution in morphometrics. *Trends in Ecology and Evolution*
1204 8:129–132.

1205 Rohlf FJ, Slice DE. 1990. Extensions of the Procrustes method for the optimal superimposition
1206 of landmarks. *Systematic Zoology* 39:40–59.
1207 Rowe TB. 1989. A new species of the theropod dinosaur *Syntarsus* from the Early Jurassic
1208 Kayenta Formation of Arizona. *Journal of Vertebrate Paleontology* 9:125–136.
1209 Sadleir RW, Barrett PM, Powell HP. 2008. The anatomy and systematics of *Eustreptospondylus*
1210 *oxoniensis*, a theropod dinosaur from the Middle Jurassic of Oxfordshire, England.
1211 *Monograph of the Palaeontological Society* 627:1–82.
1212 Sakamoto M. 2010. Jaw biomechanics and the evolution of biting performance in theropod
1213 dinosaurs. *Proceedings of the Royal Society B* 277:3327–3333.
1214 Salgado L. 1999. The macroevolution of the Diplodocimorpha (Dinosauria; Sauropoda): a
1215 developmental model. *Ameghiniana* 36:203–216.
1216 Sampson SD. 1999. Sex and destiny: the role of mating signals in speciation and
1217 macroevolution. *Historical Biology* 13:173–197.
1218 Sander PM, Klein N, Buffetaut E, Cuny G, Suteethorn V, Le Loeuff J. 2004. Adaptive radiation
1219 in sauropod dinosaurs: bone histology indicates rapid evolution of giant body size through
1220 acceleration. *Organisms, Diversity & Evolution* 4:165–173.
1221 Sander PM, Christian A, Clauss M, Fechner R, Gee CT, Griebeler EM, Gunga H-C, Hummel J,
1222 Mallison H, Perry SF, Preuschoft H, Rauhut OWM, Remes K, Tüttken T, Wings O, Witzel
1223 U. 2010. Biology of the sauropod dinosaurs: the evolution of gigantism. *Biological*
1224 *Reviews* 86:117–155.
1225 Schmitz L, Motani R. 2011. Nocturnality in dinosaurs inferred from scleral ring and orbit
1226 morphology. *Science* 332:705–708.

1227 Schoch RR. 2009. Life-cycle evolution as response to diverse lake habitats in Paleozoic
1228 amphibians. *Evolution* 63:2738–2749.
1229 Schoch RR. 2010. Heterochrony: the interplay between development and ecology exemplified by
1230 a Paleozoic amphibian clade. *Paleobiology* 36:318–334.
1231 Schoch RR. 2014. Amphibian skull evolution: the developmental and functional context of
1232 simplification, bone loss and heterotopy. *Journal of Experimental Zoology (MOL DEV*
1233 *EVOL)* 322B:619–630.
1234 Schwarz-Wings D, Böhm N. 2014. A morphometric approach to the specific separation of the
1235 humeri and femora of *Dicraeosaurus* from the Late Jurassic of Tendaguru/Tanzania. *Acta*
1236 *Palaeontologica Polonica* 59:81–98.
1237 Singleton M. 2002. Patterns of cranial shape variation in the *Papionini* (Primates:
1238 Cercopithecinae). *Journal of Human Evolution* 42:547–578.
1239 Slice DE. 2007. Geometric morphometrics. *Annual Review of Anthropology* 36:261–281.
1240 Smith KK. 1993. The form of the feeding apparatus in terrestrial vertebrates: studies of
1241 adaptation and constraint. In: Hanken J, Hall BK eds. *The skull. Vol. 3. Patterns of*
1242 *structural and systematic diversity*. Chicago: University of Chicago Press, 150–196.
1243 Smith ND, Makovicky PJ, Hammer WR, Currie PJ. 2007. Osteology of *Cryolophosaurus ellioti*
1244 (Dinosauria: Theropoda) from the Early Jurassic of Antarctica and implications for early
1245 theropod evolution. *Zoological Journal of the Linnean Society* 151:377–421.
1246 Stromer E. 1934. Die Zähne des *Compsognathus* und Bemerkungen über das Gebiß der
1247 Theropoda. *Centralblatt für Mineralogie, Geologie und Paläontologie, B* 1934:74–85.

1248 Sues H-D, Nesbitt SJ, Berman DS, Henrici AC. 2011. A late-surviving basal theropod dinosaur
1249 from the latest Triassic of North America. *Proceedings of the Royal Society B* 278:3459–
1250 3464.
1251 Tallman M, Almécija S, Reber SL, Alba DM, Moyà-Solà S. 2013. The distal tibia of
1252 *Hispanopithecus laietanus*: more evidence for mosaic evolution in Miocene apes. *Journal*
1253 *of Human Evolution* 64:319–327.
1254 Therrien F, Henderson DM. 2007. My theropod is bigger than yours...or not: estimating body
1255 size from skull length in theropods. *Journal of Vertebrate Paleontology* 27:108–115.
1256 Tortosa T, Buffetaut E, Vialle N, Dutour Y, Turini E, Cheylan G. 2013. A new abelisaurid
1257 dinosaur from the Late Cretaceous of southern France: Palaeobiogeographical
1258 implications. *Annales de Paléontologie* 100:63−86.
1259 Tsuihiji T, Watabe M, Tsogtbaatar K, Tsubamoto T, Barsbold R, Suzuki S, Lee AH, Ridgely
1260 RC, Kawahara Y, Witmer LM. 2011. Cranial osteology of a juvenile specimens of
1261 *Tarbosaurus bataar* (Theropoda, Tyrannosauridae) from the Nemegt Formation (Upper
1262 Cretaceous) of Bugin Tsav, Mongolia. *Journal of Vertebrate Paleontology* 31:497–517.
1263 Turner AH, Pol D, Clarke JA, Erickson GM, Norell MA. 2007. A basal dromaeosaurid and size
1264 evolution preceding avian flight. *Science* 317:1378–1381.
1265 Turner AH, Makovicky PJ, Norell MA. 2012. A review of dromaeosaurid systematics and
1266 paravian phylogeny. *Bulletin of the American Museum of Natural History* 371:1–206.
1267 Tykoski RS. 1998. *The osteology of* Syntarsus kayentakatae *and its implications for ceratosaurid*
1268 *phylogeny*. Austin: The University of Texas, Austin.
1269 Tykoski RS, Rowe TB. 2004. Ceratosauria. In: Weishampel DB, Dodson P, Osmólska H eds.
1270 *The Dinosauria*. Berkeley: University of California Press, 47–70.

1271 Webster AJ, Purvis A. 2002. Testing the accuracy of methods for reconstructing ancestral states
1272 of continuous characters. *Proceedings of the Royal Society of London B* 269:143–149.
1273 Werner J, Griebeler EM. 2014. Allometries of maximum growth rate versus body mass at
1274 maximum growth indicate that non-avian dinosaurs had growth rates typical of fast
1275 growing ectothermic sauropsids. *PLoS ONE* 9:e88834.
1276 Wilson JA, Sereno PC. 1998. Early evolution and higher-level phylogeny of sauropod dinosaurs.
1277 *Society of Vertebrate Paleontology Memoir* 5:1–68.
1278 Witmer LM. 1997. The evolution of the antorbital cavity of archosaurs: a study in soft-tissue
1279 reconstruction in the fossil record with an analysis of the function of pneumaticity. *Society*
1280 *of Vertebrate Paleontology Memoir* 3:1–73.
1281 Witzel U, Mannhardt J, Goessling R, Micheeli P, Preuschoft H. 2011. Finite element analyses
1282 and virtual syntheses of biological structures and their application to sauropod skulls. In:
1283 Klein N, Remes K, Gee CT, Sander PM eds. *Biology of the sauropod dinosaurs:*
1284 *understanding the life of giants*. Bloomington: Indiana University Press, 171–181.
1285 Witzel U, Preuschoft H. 2005. Finite-element model construction for the virtual synthesis of the
1286 skulls in vertebrates: case study of Diplodocus. *The Anatomical Record* 283A:391–401.
1287 Xu X, Norell MA, Kuang X, Wang X, Zhao Q, Jia C. 2004. Basal tyrannosauroids from China
1288 and evidence for protofeathers in tyrannosauroids. *Nature* 431:680–684.
1289 Xu X, Clark JM, Forster CA, Norell MA, Erickson GM, Eberth DA, Jia C, Zhao Q. 2006. A
1290 basal tyrannosauroid dinosaur from the Late Jurassic of China. *Nature* 439:715–718.
1291 Xu X, Wu X. 2001. Cranial morphology of *Sinornithosaurus millenii* Xu et al. 1999 (Dinosauria:
1292 Theropoda: Dromaeosauridae) from the Yixian Formation of Liaoning, China. *Canadian*
1293 *Journal of Earth Sciences* 38:1739–1752.

1294 Young MT, Larvan MD. 2010. Macroevolutionary trends in the skull of sauropodomorph
1295 dinosaurs - the largest terrestrial animals to have ever lived. In: Elewa AMT ed.
1296 *Morphometrics for non-morphometricans*. Berlin: Springer, 259–269.
1297 Zanno LE, Makovicky PJ. 2011. Herbivorous ecomorphology and specialization patterns in
1298 theropod dinosaur evolution. *Proceedings of the National Academy of Sciences* 108:232–
1299 237.
1300 Zelditch ML, Swiderski DL, Sheets HD. 2012. *Geometric morphometrics for biologists: a*
1301 *primer*. Amsterdam: Elsevier Academic Press.
1302

1304 **Figure and Table captions**

1305

1306 **Figure 1 Ontogenetic changes in the skull of saurischian dinosaurs**. (a) General ontogenetic
1307 pattern in Saurischia exemplified for the basal theropod *Coelophysis* (adult specimen modified
1308 after Rauhut, 2003). (b-f) Specific ontogenetic changes in saurischian dinosaurs visualized as
1309 wireframes of Procrustes-fitted shapes. (b) *Massospondylus*. (c) *Coelophysis*. (d) Megalosaurid
1310 taxon. (e) *Allosaurus*. (f) *Tarbosaurus*. Grey dashed lines represent the juvenile stage and black
1311 solid lines represent the adult stage.

1312

1313 **Figure 2 Principal component analysis of the main sample.** (a) Ontogenetic trajectories of
1314 terminal taxa for PC 1 versus PC 2. (b) Ontogenetic trajectories of terminal taxa for PC 1 against
1315 PC 3. (c) Illustration of the main shape changes for the first three principal components.
1316 Theropod taxa are shown as black dots, while sauropodomorph taxa are shown as grey dots. The
1317 arrows illustrate the different ontogenetic trajectories, in which the arrowhead marks the position
1318 of the adult individual.

1319

1320 **Figure 3 Principal component analysis of ontogenetic trajectories.** (a) Terminal and ancestral
1321 ontogenetic trajectories for PC 1 against PC 2. The arrows illustrate the different ontogenetic
1322 trajectories, in which the arrowhead marks the position of the adult individual and the base of the
1323 arrow indicates the juvenile individual. (b) Illustration of the main shape changes for the first two
1324 principal components.

1325

Figure 4 Centroid size regression analyses for the main sample. (a) Regression analysis of all terminal taxa including ontogenetic trajectories against log-transformed skull centroid size (LogCS) ($p < 0.0001$). (b) Regression analysis of only terminal (solid arrows) and ancestral (dashed arrows) ontogenetic trajectories against log centroid size ($p < 0.0001$) using the regression score as shape variable. (c) Equivalent regression analysis to (b) using the Euclidean distance as shape variable. Theropod taxa are shown as black dots, while sauropodomorph taxa are shown as grey dots. The arrows illustrate the different ontogenetic trajectories, in which the arrowhead marks the position of the adult individual and the base of the arrow indicates the juvenile individual.

Figure 5 Simplified phylogeny of Saurischia showing the main heterochronic trends of the skull. Peramorphosis is colored in green and paedomorphosis in yellow. Grey trends indicate uncertain shape trends. Shape of the hypothetical ancestors based on the continuous character mapping of the Procrustes-fitted shapes of the adult terminal taxa from the original data set. Blue skulls represent ancestral skull shapes for which ontogeny could not be analysed. The heterochronic trends found in the regression analyses are visualized by the color of the branches. Possible heterochronic trends related to the skull evolution of allosauroids and basal coelurosaurs (see discussion) are shown as dashed branches.

1346 **Table 1 Angles and length of terminal ontogenetic trajectories.** Angles of ontogenetic
1347 trajectories against PC 1, pairwise angles between ontogenetic trajectories in the PC 1-PC 2 and
1348 PC 1-PC 3 morphospace and length of ontogenetic trajectories in the PC 1-PC 2 and PC 1-PC 3
1349 morphospace (Fig. 2a, b). Green fields mark pairwise angles in the PC 1-PC 2 morphospace and
1350 orange fields mark that of the PC 1-PC 3 morphospace. Angles, lengths and slopes of
1351 ontogenetic trajectories versus log-transformed centroid size (LogCS) (Fig. 4a).
1352
1353 **Table 2 Angles and lengths of terminal and ancestral ontogenetic trajectories.** Angles of
1354 ontogenetic trajectories against PC 1, pairwise angles between ontogenetic trajectories in the PC
1355 1-PC 2 morphospace and length of ontogenetic trajectories in the PC 1-PC 2 morphospace (Fig.
1356 3a).
1357
1358 **Table 3 Angles and lengths of terminal and ancestral ontogenetic trajectories.** Angles,
1359 lengths and slopes of ontogenetic trajectories from the regression of shape (Regression score, RS
1360 and Euclidean Distance, ED) versus log-transformed centroid size (LogCS) (Fig. 4b, c).
1361
1362 **Table 4 Overview of heterochronies in saurischian skull shape**. The differences of the
1363 regression scores (ΔRS) and the Euclidean distances (ΔED) between ancestor-descendent
1364 relationships of adult individuals from the regression analysis (Fig. 4b, c) and the interpretation
1365 regarding heterochrony. ΔRS and ΔED values in brackets mark insignificant trends. NA = not
1366 available.

Table 1(on next page)

Angles and length of terminal ontogenetic trajectories

Angles of ontogenetic trajectories against PC 1, pairwise angles between ontogenetic trajectories in the PC 1-PC 2 and PC 1-PC 3 morphospace and length of ontogenetic trajectories in the PC 1-PC 2 and PC 1-PC 3 morphospace (Fig. 2a, b). Green fields mark pairwise angles in the PC 1-PC 2 morphospace and orange fields mark that of the PC 1-PC 3 morphospace. Angles, lengths and slopes of ontogenetic trajectories versus log-transformed centroid size (LogCS) (Fig. 4a).

Table 1 Angles and length of terminal ontogenetic trajectories. Angles of ontogenetic trajectories against PC 1, pairwise angles between ontogenetic trajectories in the PC 1-PC 2 and PC 1-PC 3 morphospace and length of ontogenetic trajectories in the PC 1-PC 2 and PC 1-PC 3 morphospace (Fig. 2a, b). Green fields mark pairwise angles in the PC 1-PC 2 morphospace and orange fields mark that of the PC 1-PC 3 morphospace. Angles, lengths and slopes of ontogenetic trajectories versus log-transformed centroid size (LogCS) (Fig. 4a).

	Massospondylus	***Coelophysis***	**Megalosaurid taxon**	***Allosaurus***	***Tarbosaurus***
Angle (PC 1-PC 2)	85.6492	42.3458	83.3216	5.3228	3.7406
Length (PC 1-PC 2)	0.1761	0.1174	0.1414	0.0332	0.0403
Angle (PC 1-PC 3)	63.2316	10.1684	65.0464	18.5268	60.5157
Length (PC 1-PC 3)	0.0297	0.0881	0.0390	0.0349	0.0818
	Massospondylus	***Coelophysis***	**Megalosaurid taxon**	***Allosaurus***	***Tarbosaurus***
Massospondylus	0	73.4000	128.2780	98.2417	177.2841
Coelophysis	43.3033	0	54.8780	171.6416	109.3159
Megalosaurid taxon	2.3276	40.9757	0	133.4803	54.4379
Allosaurus	89.0280	132.3313	91.3556	0	79.0425
Tarbosaurus	98.0914	141.3947	100.4190	9.0634	0
	Massospondylus	***Coelophysis***	**Megalosaurid taxon**	***Allosaurus***	***Tarbosaurus***
Angle (LogCS)	3.3947	4.8961	4.6105	0.2535	1.5851
Length (LogCS)	2.2815	1.0636	1.8147	1.0657	1.4016
Slope (LogCS)	0.0593	0.0857	0.0806	0.0044	0.0277

Table 2(on next page)

Angles and lengths of terminal and ancestral ontogenetic trajectories

Angles of ontogenetic trajectories against PC 1, pairwise angles between ontogenetic trajectories in the PC 1-PC 2 morphospace and length of ontogenetic trajectories in the PC 1-PC 2 morphospace (Fig. 3a).

Table 2 Angles and lengths of terminal and ancestral ontogenetic trajectories. Angles of ontogenetic trajectories against PC 1, pairwise angles between ontogenetic trajectories in the PC 1-PC 2 morphospace and length of ontogenetic trajectories in the PC 1-PC 2 morphospace (Fig. 3a).

	Saurischia	*Massospondylus*	Neotheropoda	*Coelophysis*	Orionides	Megalosaurid taxon	Avetheropoda	*Allosaurus*	*Tarbosaurus*
Angle (PC 1-PC 2)	29.5357	15.193	19.6691	4.0256	33.2773	35.5725	29.4664	65.5478	79.1993
Length (PC 1-PC 2)	0.082	0.1372	0.1202	0.1162	0.0879	0.1571	0.0429	0.044	0.0735
	Saurischia	***Massospondylus***	**Neotheropoda**	***Coelophysis***	**Orionides**	**Megalosaurid taxon**	**Avetheropoda**	***Allosaurus***	***Tarbosaurus***
Saurischia	0								
Massospondylus	14.3427	0							
Neotheropoda	9.8666	4.4761	0						
Coelophysis	25.5101	11.1674	15.6435	0					
Orionides	3.7416	18.0843	13.6082	29.2517	0				
Megalosaurid taxon	6.0368	20.3795	15.9034	31.5469	2.2952	0			
Avetheropoda	0.0693	14.2734	9.7973	25.4408	3.8109	6.1061	0		
Allosaurus	84.9165	99.2591	94.783	110.4266	81.1749	78.8797	84.9858	0	
Tarbosaurus	71.265	85.6076	81.1315	96.7751	67.5234	65.2282	71.3343	13.6515	0

Table 3(on next page)

Angles and lengths of terminal and ancestral ontogenetic trajectories

Angles, lengths and slopes of ontogenetic trajectories from the regression of shape (Regression score, RS and Euclidean Distance, ED) versus log-transformed centroid size (LogCS) (Fig. 4b, c).

Table 3 Angles and lengths of terminal and ancestral ontogenetic trajectories. Angles, lengths and slopes of ontogenetic trajectories from the regression of shape (Regression score, RS and Euclidean Distance, ED) versus log-transformed centroid size (LogCS) (Fig. 4b, c).

Regression (RS)	**Saurischia**	***Massospondylus***	**Neotheropoda**	***Coelophysis***	**Orionides**	**Megalosaurid taxon**	**Avetheropoda**	***Allosaurus***	***Tarbosaurus***
Angle (LogCS)	4.3762	3.8814	5.1181	6.056	4.1743	5.029	3.0083	1.1845	0.7153
Length (LogCS)	1.1084	2.2828	1.3988	1.0657	1.3267	1.8158	0.9628	1.0659	1.4011
Slope (LogCS)	0.0765	0.0678	0.0896	0.1061	0.0730	0.0880	0.0526	0.0207	0.0125
Regression (ED)	**Saurischia**	***Massospondylus***	**Neotheropoda**	***Coelophysis***	**Orionides**	**Megalosaurid taxon**	**Avetheropoda**	***Allosaurus***	***Tarbosaurus***
Angle (LogCS)	3.4145	5.0440	4.0199	5.0905	2.7768	3.4451	1.7014	-0.1758	-0.1087
Length (LogCS)	1.1071	2.2864	1.3967	1.0640	1.3248	1.8121	0.9619	1.0657	1.4010
Slope (LogCS)	0.0597	0.0883	0.0703	0.0891	0.0485	0.0602	0.0297	-0.0031	-0.0019

Table 4(on next page)

Overview of heterochronies in saurischian skull shape

The differences of the regression scores (ΔRS) and the Euclidean distances (ΔED) between ancestor-descendent relationships of adult individuals from the regression analysis (Fig. 4b, c) and the interpretation regarding heterochrony. ΔRS and ΔED values in brackets mark insignificant trends. NA = not available.

Table 4 Overview of heterochronies in saurischian skull shape. The differences of the regression scores (ΔRS) and the Euclidean distances (ΔED) between ancestor-descendent relationships of adult individuals from the regression analysis (Fig. 4b, c) and the interpretation regarding heterochrony. ΔRS and ΔED values in brackets mark insignificant trends. NA = not available.

	ΔRS	ΔED	Heterochrony
Saurischia-*Massospondylus*	-0.0262	-0.0446	Paedomorphosis
Saurischia-Neotheropoda	0.0629	0.0733	Peramorphosis
Neotheropoda-*Coelophysis*	0.0140	0.0668	Peramorphosis
Neotheropoda-Orionides	0.0146	(-0.0079)	NA
Orionides-megalosaurid taxon	0.0507	0.0497	Peramorphosis
Orionides-Avetheropoda	-0.0299	-0.0256	Paedomorphosis
Avetheropoda-*Allosaurus*	0.0153	(0.0066)	NA
Avetheropoda-*Tarbosaurus*	-0.0145	(0.0015)	NA
95 % CIs	0.0078	0.0098	
Significance levels (p=0.05)	0.0117	0.0147	

1

Ontogenetic changes in the skull of saurischian dinosaurs

(a) General ontogenetic pattern in Saurischia exemplified for the basal theropod *Coelophysis* (adult specimen modified after Rauhut, 2003). (b-f) Specific ontogenetic changes in saurischian dinosaurs visualized as wireframes of Procrustes-fitted shapes. (b) *Massospondylus*. (c) *Coelophysis*. (d) Megalosaurid taxon. (e) *Allosaurus*. (f) *Tarbosaurus*. Grey dashed lines represent the juvenile stage and black solid lines represent the adult stage.

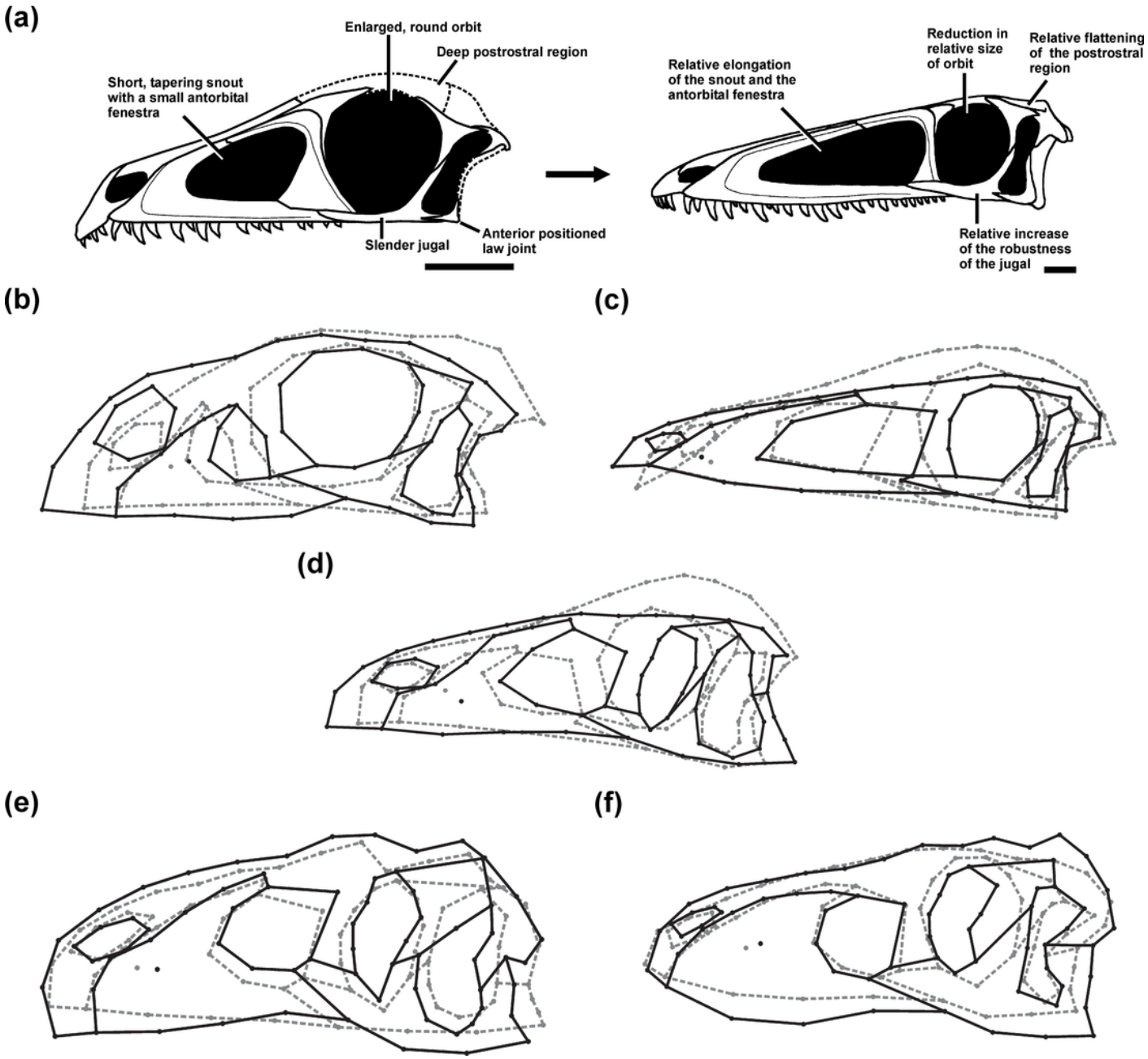
(a)
Enlarged, round orbit
Deep postrostral region
Short, tapering snout with a small antorbital fenestra
Slender jugal
Anterior positioned law joint
Relative elongation of the snout and the antorbital fenestra
Reduction in relative size of orbit
Relative flattening of the postrostral region
Relative increase of the robustness of the jugal
(b)
(c)
(d)
(e)
(f)

2

Principal component analysis of the main sample

(a) Ontogenetic trajectories of terminal taxa for PC 1 versus PC 2. (b) Ontogenetic trajectories of terminal taxa for PC 1 against PC 3. (c) Illustration of the main shape changes for the first three principal components. Theropod taxa are shown as black dots, while sauropodomorph taxa are shown as grey dots. The arrows illustrate the different ontogenetic trajectories, in which the arrowhead marks the position of the adult individual.

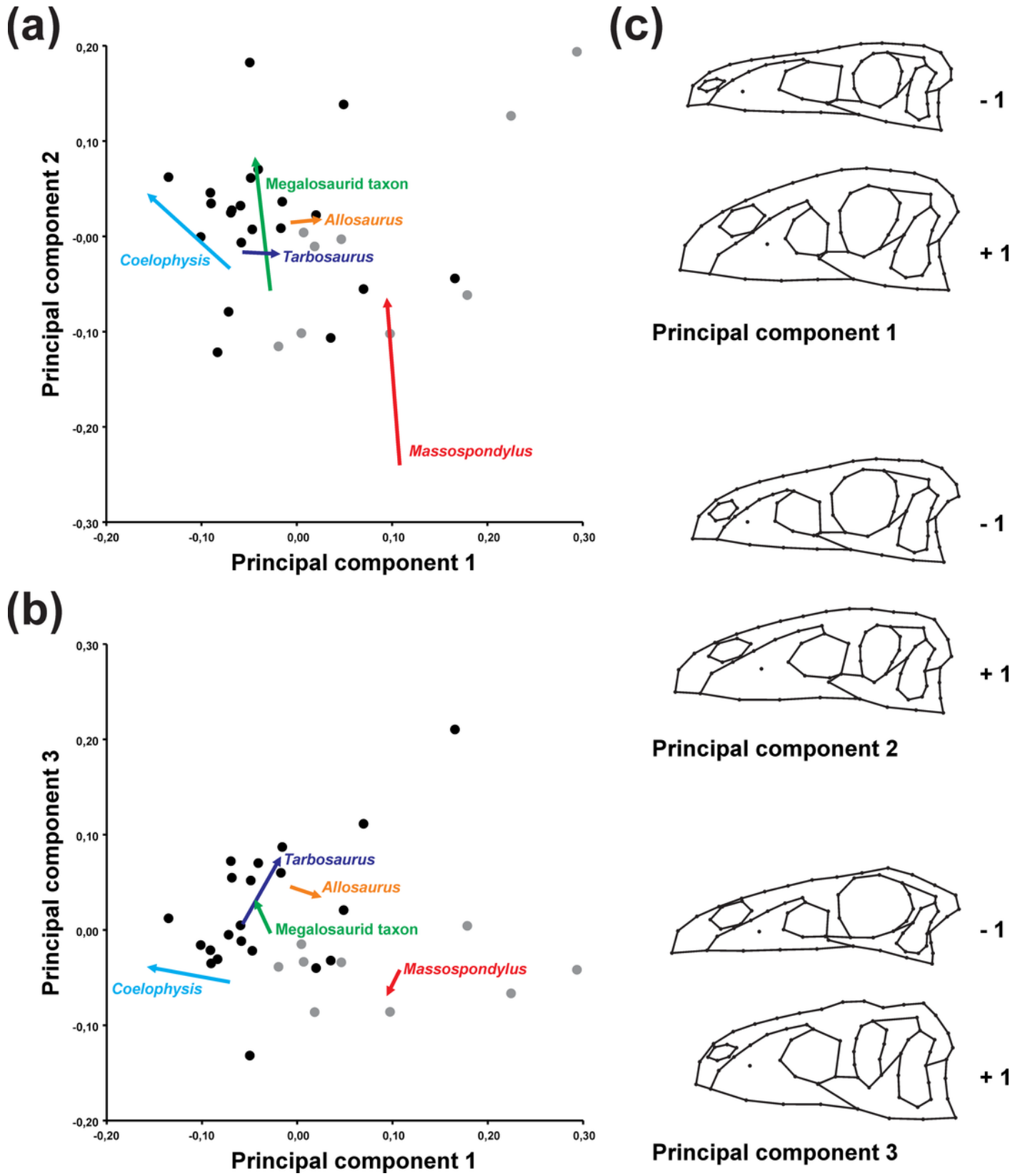
(a)
Principal component 2
Principal component 1
Megalosaurid taxon
Allosaurus
Tarbosaurus
Coelophysis
Massospondylus
(b)
Principal component 3
Principal component 1
Tarbosaurus
Allosaurus
Megalosaurid taxon
Massospondylus
Coelophysis
(c)
- 1
+ 1
Principal component 1
- 1
+ 1
Principal component 2
- 1
+ 1
Principal component 3

3

Principal component analysis of ontogenetic trajectories

(a) Terminal and ancestral ontogenetic trajectories for PC 1 against PC 2. The arrows illustrate the different ontogenetic trajectories, in which the arrowhead marks the position of the adult individual and the base of the arrow indicates the juvenile individual. (b) Illustration of the main shape changes for the first two principal components.

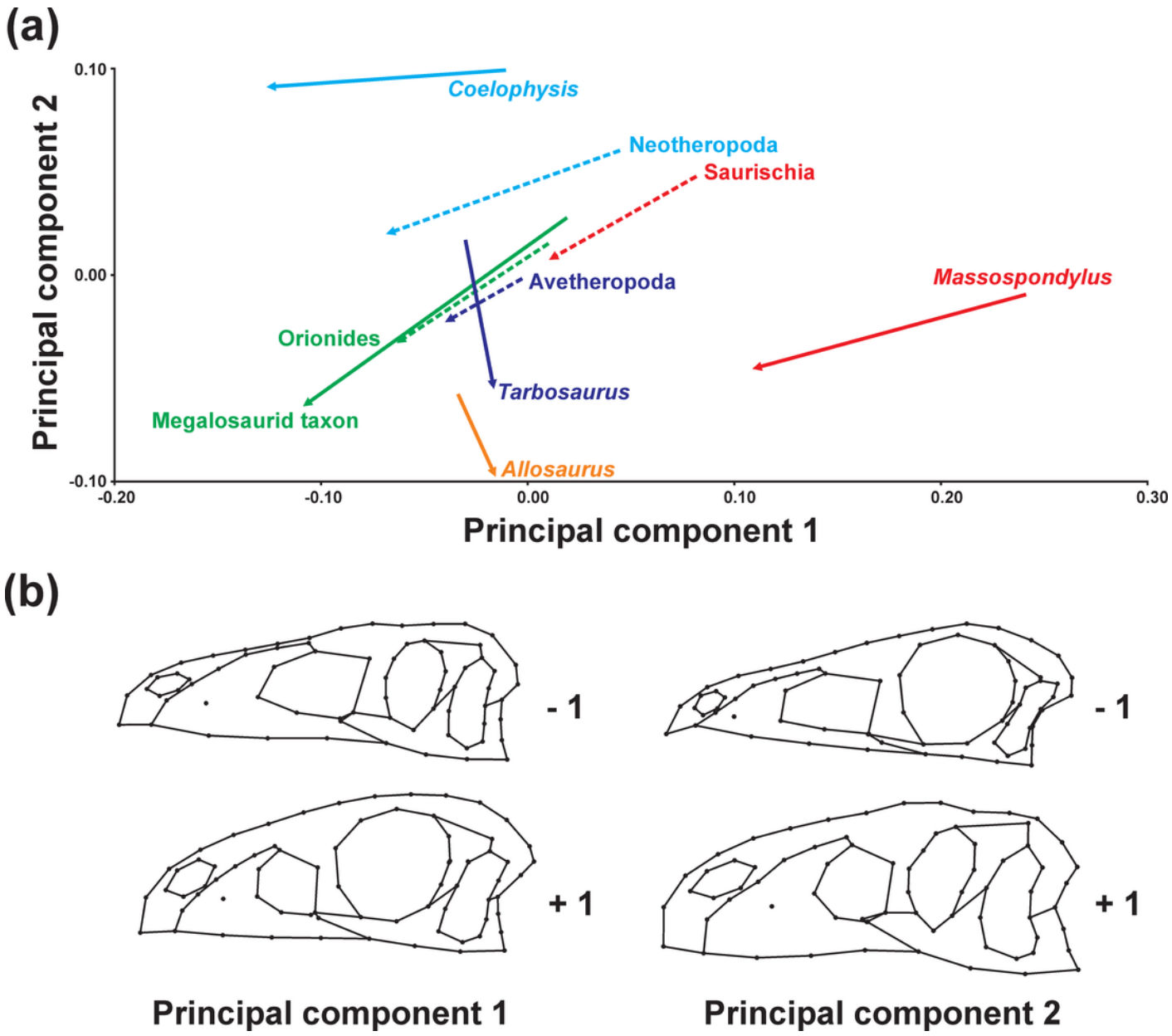

4

Centroid size regression analyses for the main sample

(a) Regression analysis of all terminal taxa including ontogenetic trajectories against log-transformed skull centroid size (LogCS) ($p < 0.0001$). (b) Regression analysis of only terminal (solid arrows) and ancestral (dashed arrows) ontogenetic trajectories against log centroid size ($p < 0.0001$) using the regression score as shape variable. (c) Equivalent regression analysis to (b) using the Euclidean distance as shape variable. Theropod taxa are shown as black dots, while sauropodomorph taxa are shown as grey dots. The arrows illustrate the different ontogenetic trajectories, in which the arrowhead marks the position of the adult individual and the base of the arrow indicates the juvenile individual.

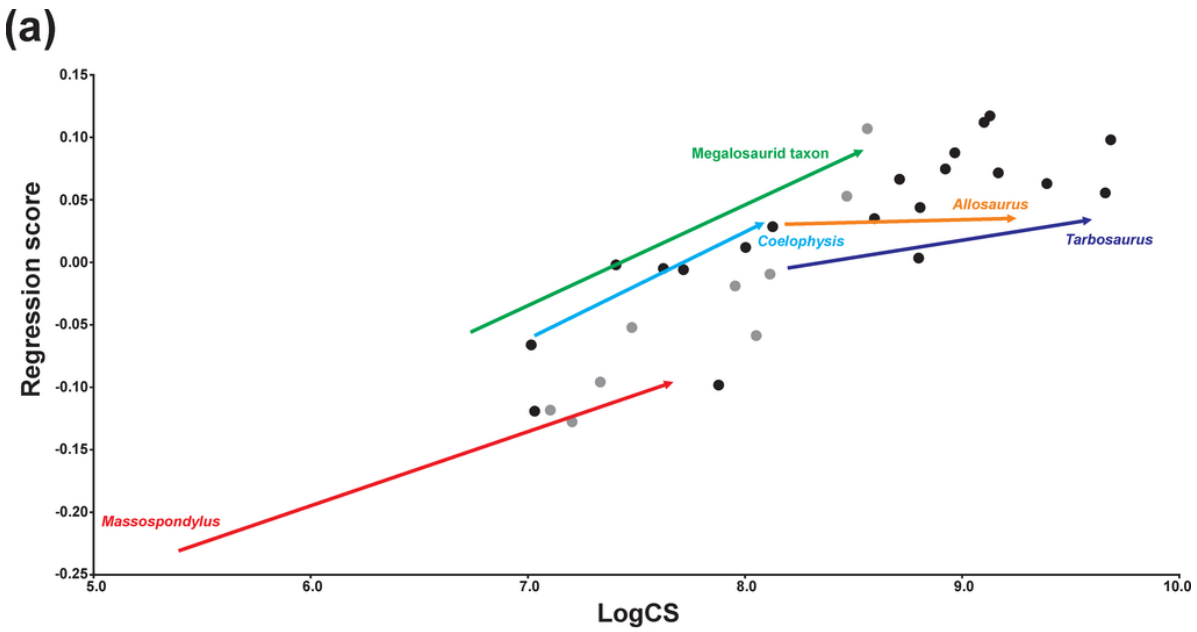
(a)
Regression score
LogCS
Megalosaurid taxon
Allosaurus
Coelophysis
Tarbosaurus
Massospondylus

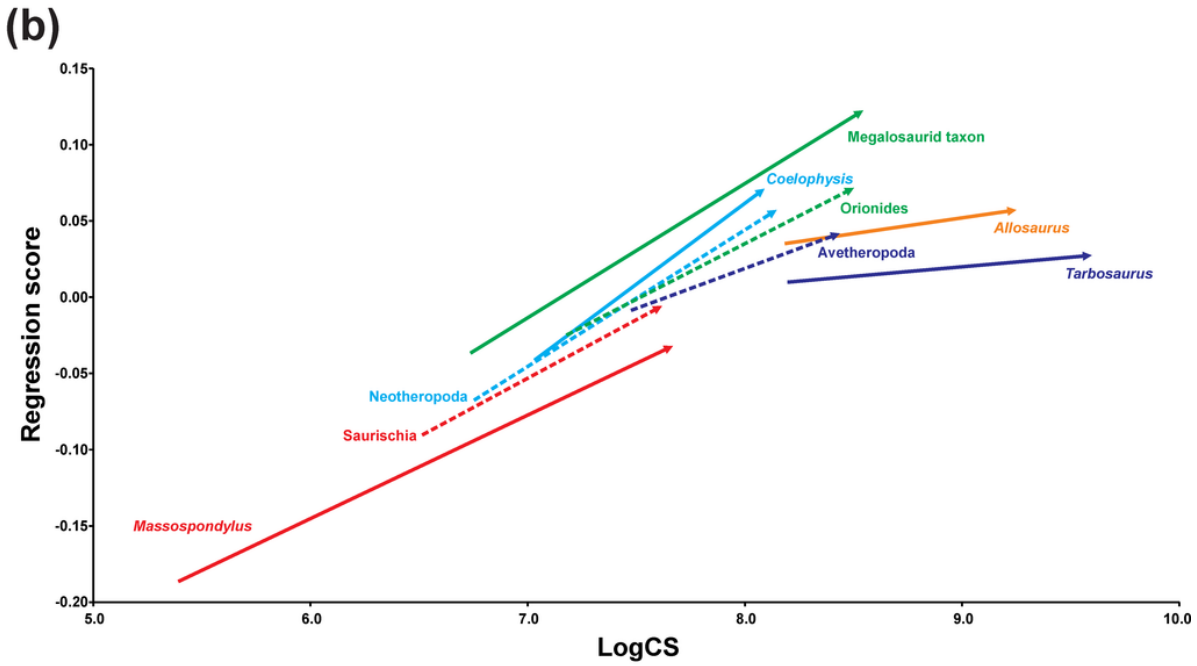
(b)
Regression score
LogCS
Megalosaurid taxon
Coelophysis
Orionides
Allosaurus
Avetheropoda
Tarbosaurus
Neotheropoda
Saurischia
Massospondylus

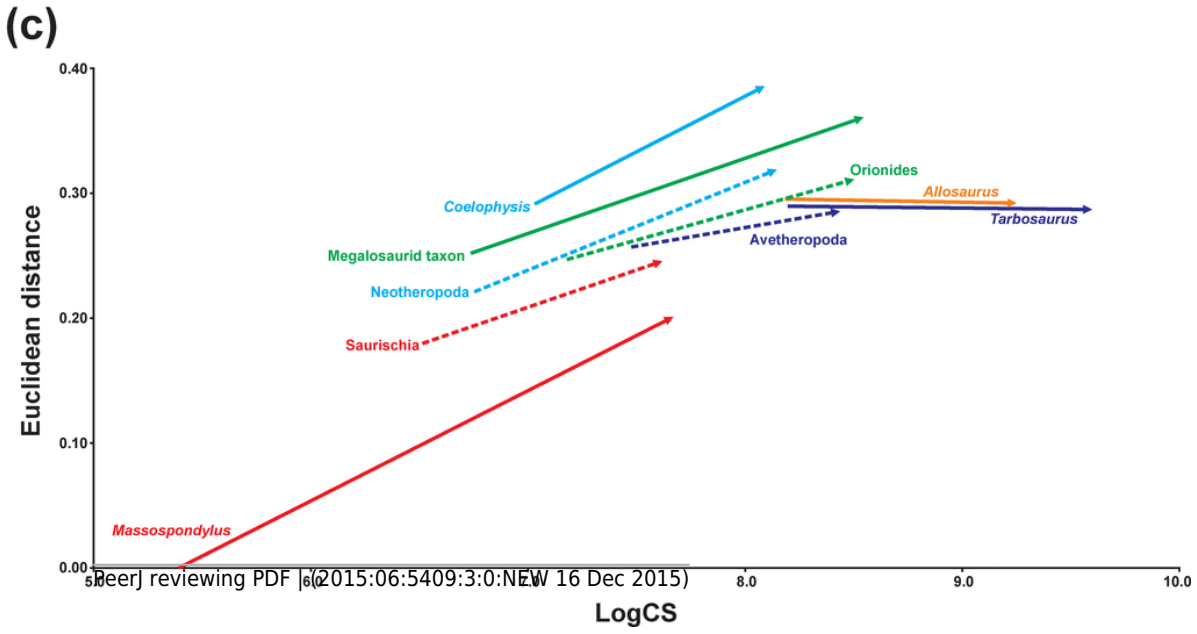
(c)
Euclidean distance
LogCS
Coelophysis
Orionides
Allosaurus
Tarbosaurus
Megalosaurid taxon
Avetheropoda
Neotheropoda
Saurischia
Massospondylus

5

Simplified phylogeny of Saurischia showing the main heterochronic trends of the skull

Peramorphosis is colored in green and paedomorphosis in yellow. Grey trends indicate uncertain shape trends. Shape of the hypothetical ancestors based on the continuous character mapping of the Procrustes-fitted shapes of the adult terminal taxa from the original data set. Blue skulls represent ancestral skull shapes for which ontogeny could not be analysed. The heterochronic trends found in the regression analyses are visualized by the color of the branches. Possible heterochronic trends related to the skull evolution of allosauroids and basal coelurosaurs (see discussion) are shown as dashed branches.

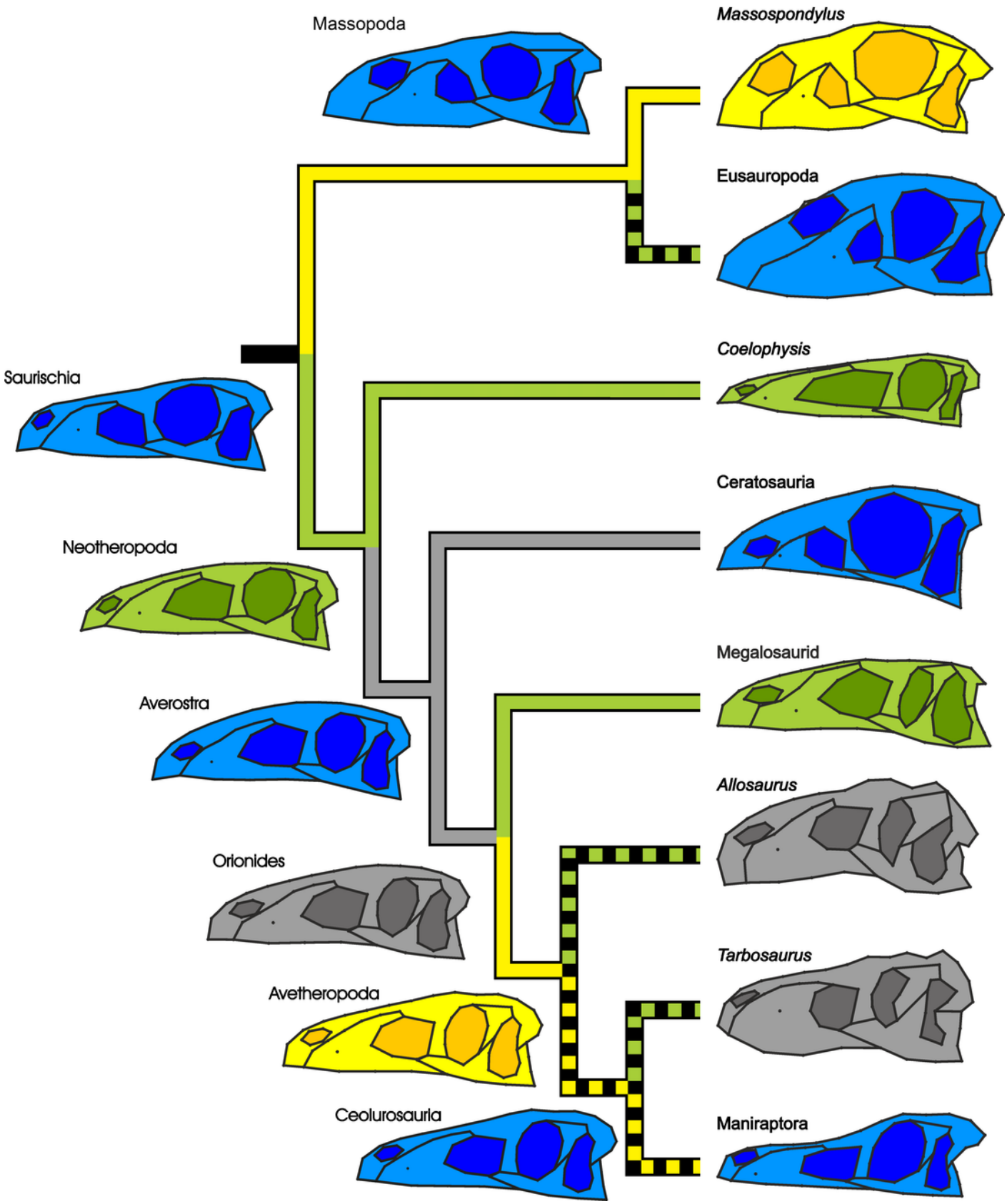
Massopoda
Massospondylus
Eusauropoda
Coelophysis
Saurischia
Ceratosauria
Neotheropoda
Megalosaurid
Averostra
Allosaurus
Orionides
Tarbosaurus
Avetheropoda
Ceolurosauria
Maniraptora